Desiccation and Cracking Behaviour of Clay Under Wetting and Drying

Adebayo Iyanuoluwa Olude

Submitted to the
Institute of Graduate Studies and Research
in partial fulfillment of the requirements for the degree of

Master of Science
in
Civil Engineering

Eastern Mediterranean University
September 2020
Gazimağusa, North Cyprus

Approval of the Institute of Graduate Studies and Research

Prof. Dr. Ali Hakan Ulusoy
Director

I certify that this thesis satisfies the requirements as a thesis for the degree of Master of Science in Civil Engineering.

Prof. Dr. Umut Türker
Chair, Department of Civil Engineering

We certify that we have read this thesis and that in our opinion it is fully adequate in scope and quality as a thesis for the degree of Master of Science in Civil Engineering.

Prof. Dr. Zalihe Nalbantoğlu Sezai
Supervisor

Examining Committee

1. Prof. Dr. Zalihe Nalbantoğlu Sezai
2. Asst. Prof. Dr. Mohammad Reza Golhashem
3. Asst. Prof. Dr. Eriş Uygar

ABSTRACT

Cracks are formed when moisture loss in soil creates channels for water flow. This research investigates the cracking behavior of clayey soil subjected to wetting-drying cycles. Laboratory tests were performed on both natural (control soil) and bentonite added soils. Desiccation rates were observed and recorded for soil specimens using the air-dry and oven-dry approach at 60^{o}C. Soil specimens containing different percentages of bentonite (5% and 10%) were subjected to four wetting and drying cycles. Double punch test was conducted to determine the tensile strength of natural soil. The swelling and shrinkage tests were carried out on natural soil specimens as well as examining the matric suction. Results of the desiccation method employed showed that cracks did not occur on the natural soil at any stage of the air-drying condition while in the oven-drying method, cracks were observed in the increasing drying stages. Crack dimension was quantified by using digital image processing known as ImageJ software. The results for the experimental cyclic wetting and drying indicated that the crack intensity factor, CIF increased with an increasing number of cycles. Soil water characteristic curve, SWCC of the control soil was constructed using filter paper method and the air-entry value, AEV was obtained at 31% water content. This water content obtained from the SWCC is in good harmony with the value obtained using the silica gel drying method.

Keywords: Air entry value, bentonite, crack intensity factor, desiccation, soil water characteristic curve, swelling and shrinkage, wetting and drying.

ÖZ

Topraktaki nem kaybı su akışı için kanallar oluşturduğunda çatlaklar oluşur. Bu araştırma, ıslatma-kurutma döngülerine maruz kalan killi toprağın çatlama davranışını incelemektedir. Hem doğal (kontrol toprağı) hem de bentonit katkılı topraklarda laboratuar testleri yapılmıştır. 60^{o}C'de hava ile kurutma ve fırında kurutma yaklaşımı kullanılarak toprak numuneleri için kuruma oranları gözlemlenmiş ve kaydedilmiştir. Farklı oranlarda bentonit (% 5 ve% 10) içeren toprak numuneleri dört ıslatma ve kurutma döngüsüne tabi tutulmuştur. Doğal toprağın çekme dayanımını belirlemek için çift vuruş testi yapılmıştır. Şişme ve büzülme testleri, doğal toprak numunelerinde ve ayrıca matrik emiş ölçülerek yapılmıştır. Kullanılan kurutma yönteminin sonuçları, doğal toprakta hava ile kurutma koşulunun hiçbir aşamasında çatlak oluşmadığını, fırında kurutma yönteminde ise artan kurutma aşamalarında çatlaklar olduğunu göstermiştir. Çatlak boyutu, ImageJ yazılımı olarak bilinen dijital görüntü işleme kullanılarak ölçüldü. Deneysel döngüsel ıslatma ve kurutma sonuçları, çatlak yoğunluğu faktörünün, CIF'in artan sayıda döngü ile arttığını gösterdi. Kontrol toprağının toprak su karakteristik eğrisi, SWCC'si filtre kağıdı yöntemi kullanılarak oluşturulmuş ve %31 su içeriğinde hava giriş değeri, AEV elde edilmiştir. SWCC'den elde edilen bu su içeriği, silika jel kurutma yöntemi kullanılarak elde edilen değer ile iyi bir uyum içerisindedir.

Anahtar Kelimeler: Hava giriş değeri, bentonit, çatlak yoğunluk faktörü, kuruma, toprak suyu karakteristik eğrisi, şişme ve büzülme, ıslanma ve kuruma.

ACKNOWLEDGEMENT

First and foremost, I give thanks to God almighty for the grace he has granted me. I offer my heartfelt appreciation to my supervisor. Prof. Dr. Zalihe Nalbantoğlu for the endless support, for her patience, inspiration, eagerness, and exalted knowledge. I also appreciate my family for their support and encouragement in the course of my study. I specially dedicate this to God and to my Mother for her relentless prayers. I appreciate all my colleagues Olorunsola Victor, Aria Norouzi, Dr. Roward Farah and to my fiancée Doofan Abaa for their assistance, encouragement and motivation for the dissertation.

TABLE OF CONTENTS

LIST OF TABLES

LIST OF FIGURES

Chapter 1

INTRODUCTION

1.1 Background

One of the oldest building materials on earth is the clay soil. They are complex natural materials, whose particle size is less than 0.002 mm. It is important in geotechnical engineering because of their complex behaviour. Quite a number of population in our societies live in structures constructed with clay which serve as an essential load bearing structures e.g buildings, earth dams, roads etc. The clay materials when used in construction possesses varying degrees of plasticity. Typically, clay soil swells when it absorbs moisture and shrinks when it loses moisture. In geotechnical engineering, cracks create weakness in soil by an increase in the compressibility which reduces the soil strength and stability (Yesiller *et al.* 2000). Clay cracks causes the permeability of soil to increase and creates a passage of water flow and thus, causes a reduction in soil strength. The factors affecting soil cracking include; the colloidal content, arrangement of particle, *in situ* unit weight, freezing-thawing and wetting-drying (Singh, 2018). Most of the studies performed in the literature studied the swelling/shrinkage behavior of clayey soils by using different techniques. However, in the literature, there are limited number of studies which consider the effect of desiccation cracking on the swelling behavior of soils. The desiccation cracks generated in clayey soils may affect the water absorption capacity of the soil and cause volume change in characteristics of the soils. Hence, it is very important to study the effect of desiccation cracks on the volume change of clayey soils. In the present study,

a laboratory investigation was carried out to study the desiccation cracks by using different drying methods and evaluate the effect of drying on the swelling/shrinkage properties of the clayey soil.

In air drying method, no cracks were observed at any stage of the air-drying whereas in the oven-drying method, at increasing oven-drying stages, some cracks were observed in the soil specimens. In order to better observe and understand the cracks generation in the soil specimens, bentonite was added to the natural soil in different percentages and the created cracks were studied. Crack dimension was quantified by using digital image processing and the results of the tests indicated that the crack intensity factor, CIF increased with an increasing number of drying cycles.

1.2 Aim and Research Objectives

In order to appropriately capture the aim of this scientific study the following objectives are critically examined:

1. Understanding crack formation during wetting and drying cycles.
2. Analyzing the results of cracks subjected to wetting and drying cycles using image analysis techniques.
3. Measurement of soil matric suction by using the filter paper method.
4. Measurement of the tensile strength of control soil by using double punch test.
5. Analyzing the swelling and shrinkage behavior of the soil specimen.

1.3 Problem Statement

For cracks, seepage, strength and deformation of expansive soil differs from an integrated soil. The consideration of crack initiation and crack processes when studying the behavior of desiccation cracks in clay soils is very important. Random calculation approach or assumption has been used to analyze cracks in the past. (Shi,

2014). As a result of this, the means of developing and measuring cracks using software analysis initiated this study. This is considered by observation and measurement of the crack parameters.

1.4 Scope of Work

The aim of this study is to examine the desiccation cracks in soil. This is accomplished by studying previous works. In the course of this research, literature review on cracks is being discussed, methodology of various tests is introduced. Results and discussions of experimental results are presented and thereafter the conclusions as well as recommendation are stated. The thesis is categorized into five chapters, which are as follows:

In Chapter 2, literature review on crack geometry, crack patterns, crack initiation and propagation, crack cycles, image cracks and soil water characteristics curve are presented.

In Chapter 3, testing strategy, soil classification, testing methods and preparation of soil specimen are shown.

In Chapter 4, cracks subjected to wetting and drying cycles are analyzed and presented. Results of soil specimen under two conditions (air-dry and oven-dry) were examined as well as the tensile strength, matric suction, swelling and shrinkage of the soil specimen.

In Chapter 5, conclusions were made from the results obtained and recommendations are provided for further studies.

Chapter 2

LITERATURE REVIEW

2.1 Introduction

It is generally known that shrinkage leads to cracks in clay soil as a result of moisture loss (Oluwaseun, 2016). The process of measuring shrinkage is quite difficult and time consuming. As a result, various methods were developed and used for shrinkage measurement. Researchers such as (Chertkov 2005; Oleszczuk et al .2003; Chertkov et al. 2004) stated that these methods were developed using isotropy for change in height by measuring deformations (vertical and horizontal) of a shrinked soil specimen.

During shrinkage, cracks occur when soils are restrained (Mitchell, 1993). This creates negative pore pressure during drying known as soil suction. Cracking evolves into range of forms, cycles of opening and closing of soil cracks which modifies the permeability of soil (Oluwaseun, 2016).

Swelling behaviour have been studied by previous researchers which includes swelling and compressibility mechanics on expansive mixtures. (Komine and Ogata, 1994; Sivapullaiah et al., 1996; Alawaji, 1999). The effect of factors includes; initial dry density and initial moisture content were evaluated.

2.2 Crack Geometry

In order to understand the mechanism of cracks, different approaches as well as different base materials such as: long mold, circular, rectangular and field analysis had been conducted (Sánchez, 2014). Also there are numerical models set up along with conditions in inducing the crack formation.

The study reveals that if there is no restraint in a drying soil, it will shrink totally without cracking. This is dependent on the environment and properties of soil. There are two factors that controls the crack initiation; the first factor is by the distribution of tensile stress with a controlled shrinkage in the soil. For the first control, studies showed that cracks will begin where tensile stress have the utmost concentration and this occurs at the middle of drying soil (Nahlawi & Kodikara, 2006). The second factor is as a result of flaws on soil surface. At this point, the crack initiation is affected by tensile stress. Nahlawi & Kodikara (2006) stated that the flaws noticed on the specimen can be as a result of large particles, air bubble, micro cracks and surface texture. Figure 2.1 shows the effect of flaws and tensile stress on cracks initiation of a compacted soil layer.

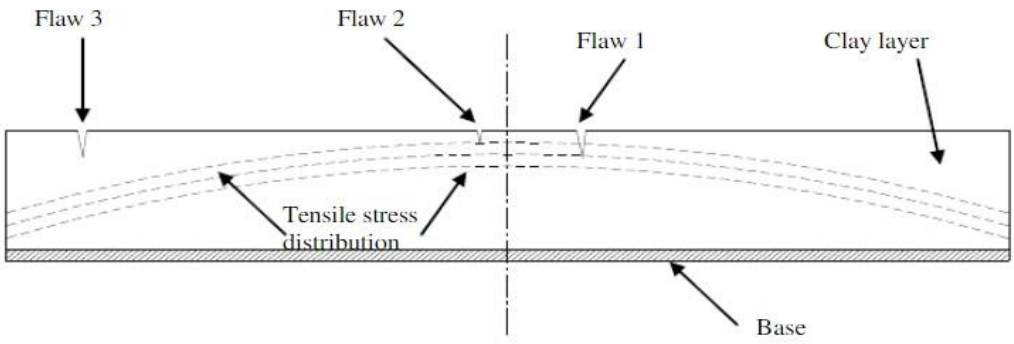

Figure 2.1: Effects of Flaws on Crack Initiation (Costa et al, 2013)

2.2.1 Type of Cracking:

In Figure 1.1, some reason for cracks could be as a result of either a change in volume or applied pressure on the soil. There are two major types of cracks as classified by Gray, (1989) with respect to its development:

1. Mechanical cracks: They are shaped through either by deposition or due to unfitting construction. An example of this type of crack is when no adequate link occurs within lifts and poor compaction.
2. Physicochemical cracks: They are categorized into three groups:
    i. Syneresis flaws.
    ii. Cracks initiated by drying the material fully.
    iii. Cracks caused by freeze-thaw cycles.

2.3 Crack Initiation and Crack Propagation

Tensile stresses exceeds the soil strength when there is loss of water (Shi, 2014). It is dependent on soil suction and water content of soil thus a crack initiates in a drying soil.

2.4 Crack Patterns

The quantification of the features that describe the pattern of the crack network is a vital aspect of cracking soils (Sánchez, 2014). The description of crack patterns is beneficial for geotechnical engineering and also in diverse areas of science and engineering (Pande, 2015). In soil mechanics, the shape, and size of structural cracks are of great importance. They have clues which can be traceable to previous strains and stresses imposed to the soil. As a result, the crack patterns may act as indicators in describing the state of the soil's structure.

Crack development using empirical formulas was determined from a typical soil investigation reports by examining formation of crack in wet soils as it relates to soil properties (Yassoglou et al. 1994). The direct technique of measurement for surface cracks was developed as an improvement (Ringrose-Voase and Sanidad 1996) over previous techniques (Dasog & Shashidhara;1993). These techniques required that crack patterns were measured manually in the field.

2.5 Mechanism of Cracking

The exposure of an expansive soil to small change in moisture content leads to change in the volume of their crack surface area (Mokhtari,2012). During precipitation, the expansion and shrinkage of soil occurs during desiccation for a drying period. According to Rao et al., (2004) water is lost through a process termed evapotranspiration. Factors that determine the change in volume are: soil compaction, clay mineral, weathering and pressure imposed on layer of soil (Mishra et al.,2008). The stages of shrinkage of a compacted soil are: initial, primary and residual shrinkage according to Mishra et al., (2008) as shown in Figure 2.2.

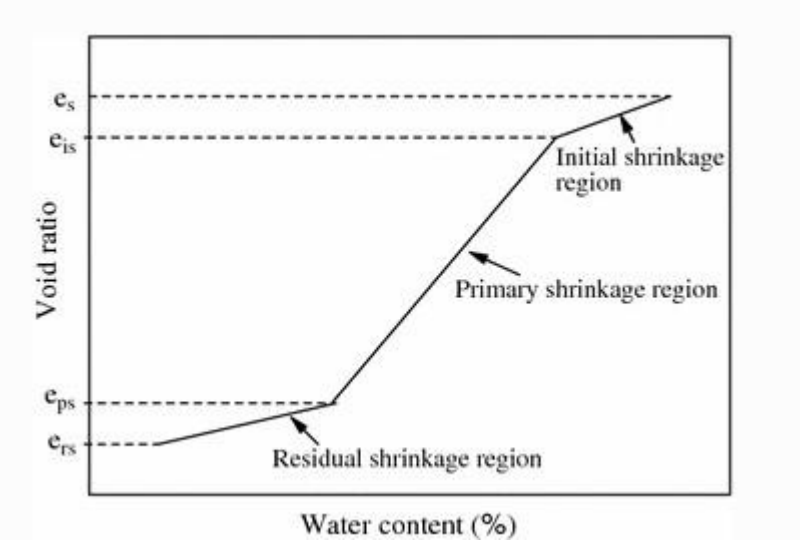

Figure 2.2: Schematic Diagram Showing the Shrinkage Regions (Mishra et al., 2008)

Soil containing different component of clay minerals undergo cracking (Novák, 1999). According to Tang et al. (2010), crack initiation and propagation is as a result of constituent particle arrangement and capillary suction. As suction increases, the component soil surface is exposed to tensile stress as evaporation evolve. The tensile stress occurs to exceed the tensile strength at this point (Shi, 2014). Hence, result in cracking (Tang et al. 2010).

There are four zones in soil shrinkage characteristics curve namely: proportional, structural, residual and zero shrinkage (Cornelis et al., 2006). They all exist for well-structured soil while structural shrinkage does not exist for clay paste (Yao et al., 2014). The extraction of large pores by biological activity is associated with structural shrinkage. It does not include significant change in volume. The proportional shrinkage phase is referred to as 'normal shrinkage' knowing that moisture reduction is equal to change in volume of geomaterials. It is important to note that throughout this stage the intra aggregate pores remain inundated (Mishra, 2019).

Desaturation begins at residual shrinkage, in which air occupies intra-aggregate pores (Hueckel, 2013). When soil water is reduced having no decrease in volume, accompanied by cracks then it is said to be at zero shrinkage stage (Cornelis et al.2006). In Figure 2.3, typical soil shrinkage characteristic curves for well-structured and non-structured soils is shown.

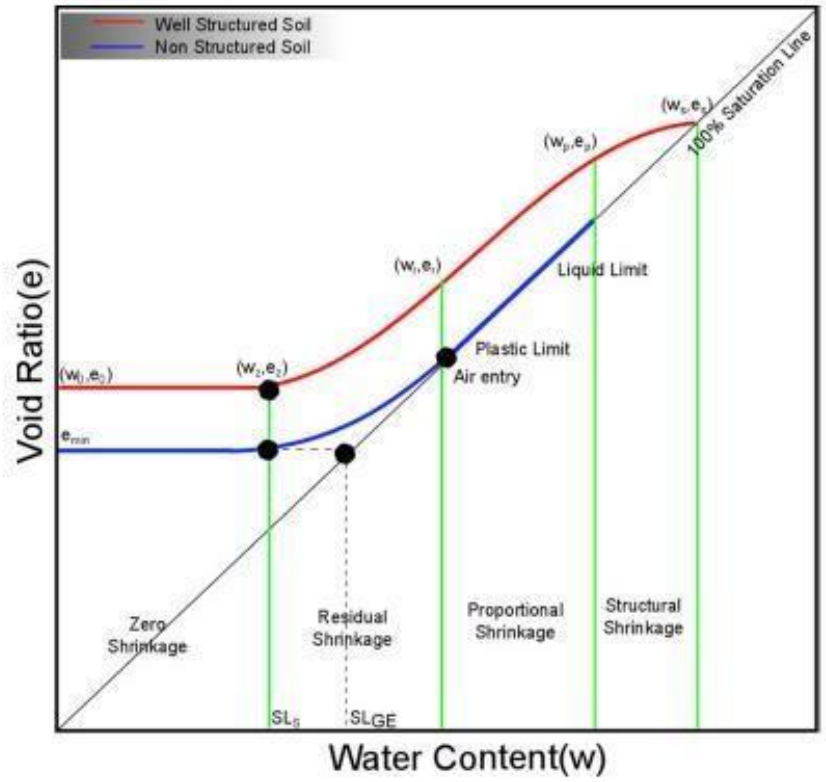

Figure 2.3: Typical Soil Shrinkage Characteristic Curve (Cornelis et al., 2006)

Generally, four zones are encountered as shown in Figure 2.3 for geomaterials namely; zero shrinkage, residual shrinkage, proportional shrinkage and structural shrinkage. All four zones occur for a well-structured soil while for non-structured soil such as; clay paste, structural shrinkage does not occur (Yao et al., 2014). The structural shrinkage is exhausting of large inter-aggregate pores and passage formed by biological activity and no significant change occurs in volume (Mishra, 2019).

The proportional shrinkage is when reduction in moisture equals change in volume of geomaterials (Mishra, 2019). Throughout this phase, intra-aggregate pores remains saturated. At the beginning of residual shrinkage, desaturation begins at the point where air enters into the intra-aggregate pores. The air entry point correlates with plastic limit of soil (Fredlund et al., 2011). Zero shrinkage is the loss of moisture without reduction in volume and indicate the forms of cracks (Cornelis et al., 2006).

The shrinkage limit is the water content at which no further volume reduction occurs as moisture loss evolves. It is obtained at an intersection of the saturation line and extension line of zero shrinkage of the shrinkage curve (Wijaya and Leong, 2014).

2.6 Image Cracks

In recent times, image-based study used to measure development of cracks with adequate accuracy is influenced by the characteristics of soil and environmental conditions (Tang et al. 2011). In this study, cracks are measured as crack density factor and crack intensity factor. According to some researchers, they defined crack density factor (CDF) as the sum total of crack areas to surface cracked area for a drying sample (Miller *et al.,* 1998; Lakshmikantha *et al.,* 2009). Miller et al., (1998) defined Crack Intensity Factor, CIF as the percentage of crack areas to whole area of specimen. The CIF is measured by saturated soils first, then undergo either oven dry or air dry conditions, thus leading to easily identifiable large cracks on surface specimen. Equation for CIF and CDF are shown below. Figure 2.4 shows the diagrammatic flow of image analysis.

$$\text{CIF} = \left\{ \frac{\text{Cracked area}}{\text{Specimen area}} \right\} \text{ x } 100 \tag{1}$$

$$\text{CDF} = \left\{ \frac{\text{Shrinkage area + Cracked area}}{\text{Initial specimen}} \right\} \text{ x } 100 \tag{2}$$

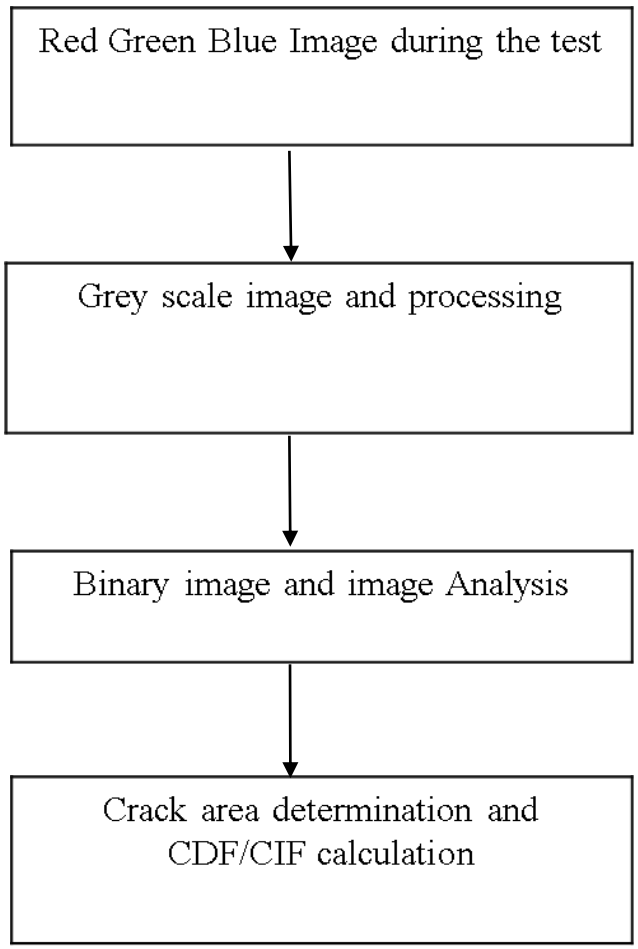

Figure 2.4: Diagramatic Flow of Image Analysis

In terms of measurement, the volumetric shrinkage strain describes the relationship between volume of soil specimen and the initial shrinkage volume. Three expansive soil specimens with different water content were examined digitally and manually by (Puppala *et al.* 2004). It was noticed that digital means displayed greater strain. Peng *et al.* (2006) set up a method for non-destructive and quantifiable measurement of shrinkage and observed the ratio of volume of crack to water loss in saturated soil. The measurement for volumetric shrinkage strain was observed digitally and manually by Oren et al. (2006).

The result of plasticity index on the crack parameters, thickness and drying temperature was observed by Tang *et al.* (2008). It was found that these parameters

gradually increase with increase in soil plasticity, temperature and sample thickness. Though, by increasing wetting-drying cycles, the crack parameters were found to decrease (Singh, 2018). Lakshmikantha et al. (2009) carried out a study on the formation and propagation of cracks. This occurrence of desiccation of soil and the image analysis helps to determine the final crack pattern. Also, palm fibre content was added with clay in order to measure swelling and shrinkage properties (Azadegan *et al.* 2012). It was observed that increase in palm fibre content shows that cracks were completely distributed instead of the long, deep and wide crack.

2.7 Crack Cycles

There has been a lot of research executed on the effects and performance of soil behavior on wetting-drying (Oluwaseun, 2016). Anderson et al. (1982) examined some laboratory test and field studies on the result of shrinkage on groundwater pressure and strength of clay earthwork. It was observed that the most prevailing cracks occurred in eight months. There was a heavy rainfall that reduced these crack depths which continued to decline until the end of the same year. By the second month of the following year, cracks closed up after another heavy rainfall.

The influence of wetting-drying cycles on the hydraulic conductivity of compacted clays was examined according to Albrecht & Benson (2001). It was noted that clay samples were compacted to an optimum water content which led to a rise in the hydraulic conductivity but a decrease when specimen were dried. Furthermore, Albrecht & Benson (2001) observed causes of desiccation on compacted clays and examined the properties of soil. The compaction conditions, mineral constituent and effects of drying on desiccation and shrinkage leads to cracking (Albrecht & Benson, 2001).

A laboratory experiment was performed by investigating the effects of wetting -drying cycles on crack initiation using clay sample in a slurry state (Tang et al., 2011). In the course of this study, four prepared slurry clay specimen undergo five cycles (wetting and drying). Factors such as crack initiation, rate of evaporation and changes in specimen structure were observed. Also crack patterns formed were examined using image processing. From the experimental observation, the ratio of crack surface, the measured cracking moisture content (the first crack that appears corresponding to the water content within the specimen) and all specimen thickness increased significantly after the first three cycles and later reached equilibrium. After the second drying cycles, the cracks formed were more irregular than the first cycle. It was noticed that the wetting-drying cycles led to the change of specimen structure as the initial homogeneous structure was altered to a clear and aggregated structures with visible aggregate pores. The volume of specimen increases with cumulative cycles as porosity increases. The setup and desiccation specimen for the research is in Figure 2.5.

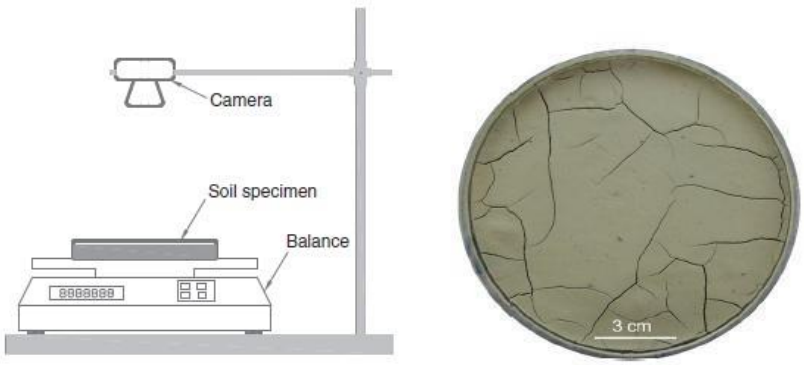

(a) (b)

Figure 2.5: (a) Schematic Diagram of Image Analysis (b) A Typical Desiccation Crack Pattern (Tang et.al, 2011)

2.8 Soil Suction

Soil suction acts as an important part in sustaining the strength of especially unsaturated slopes (Gavin, 2009; Jotisankasa, 2010). The void in soil is full of water for saturated conditions having an insignificant percentage of blocked air. In these conditions, pore water pressure has a positive value and it is considered to be hydrostatic. (Ridley, 2004) stated that the combination of molecular forces and physicochemical properties between soil and water properties form a small void within soil. In this type of attraction, the soil suction is defined by the complex energy that creates the interaction between soil, water and air present in the soil (Yong, 1999). The capillary effect allows tensile stress within the soil to absorb water from water table by filling void spaces. This serves as an obstacle by preventing water from permeating the soil thus allowing water to infiltrate into empty pore spaces.

Figure 2.6, focuses only on the effect of air entry value (AEV) which is the matric suction once bulk water is extracted from the voids in soil. The point at which air enters the pores in the soil is the air entry value signifying suction value. However, the moisture content at which the suction is vital to extract water from soil is known as residual water content. (Fredlund and Xing, 1994).

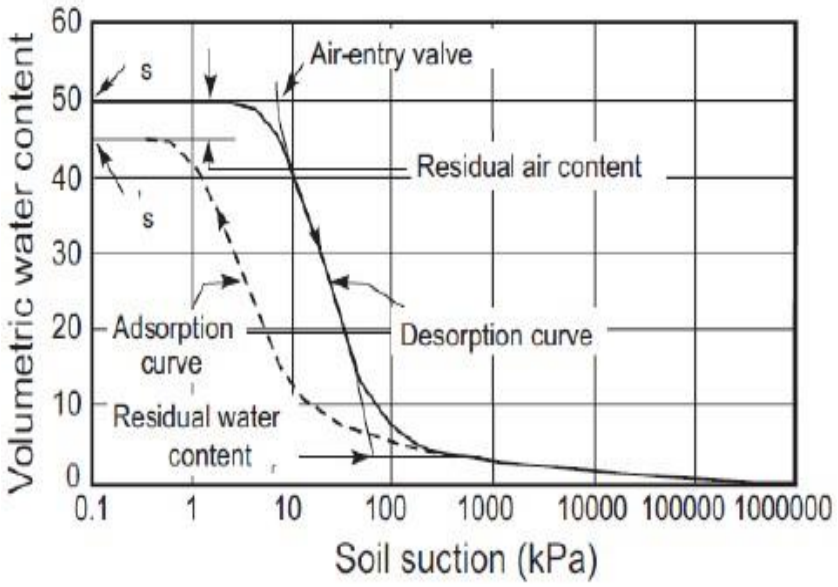

Figure 2.6: Typical Soil-water Characteristic Curve (Fredlund and Xing, 1994)

Soil suction is defined as a tiny state that reveals the degree of water attracted by the soil (Ridley et al. 2003; Sreedeep & Singh 2006). The osmotic and matric are the two components of suction. The osmotic suction occurs in pore fluid because of dissolved salts present in it while matric suction is a fine and rigorous occurrence owing to capillary texture, nature and a vital variable in the hydromechanical behavior of unsaturated soils (Vander, 2014). The total of two components; matric and osmotic suction are equal to total suction. The correlation between matric and total suctions according to Chen (1998) is described by isothermal needs in the equation below:

$$h_t = h_o + h_m \quad (3)$$

where h_t = total suction, h_o = osmotic suction and h_m = matric suction. It is observed that engineering-related problems are as a result of partially saturated soils. In other words, the tiny particles between voids are incompletely occupied with water and air. Thus, leading to negative pore water pressure that affects the stress structure (Horn, 2002). The precise amount and analysis of soil suction is required to understand unsaturated soil behavior.

2.9 Soil Water Characteristic Curve

This is the relationship between the moisture content and suction. It is important in unsaturated soil (Fredlund, 2002). Originally, moisture content is determined by a measure of in situ soil suction. The unsaturated soil properties used indirect method which includes shear strength, unsaturated permeability and change in volume. It takes time and is expensive to measure in the laboratories (Fredlund, 2002). The SWCC consist of air entry value (AEV) and the residual matric suction.

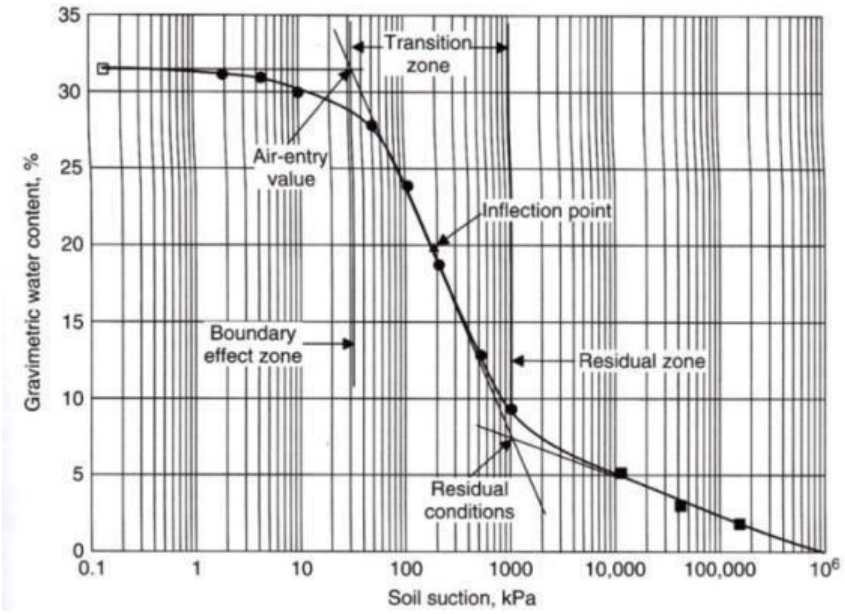

Figure 2.7: Schematical Representation of Zones in SWCC (Fredlund, 2012)

While drying from saturated conditions as shown in Figure 2.7, SWCC has two breaking point known as air entry and residual point. The air entry is the point at which soil begins to desaturate and becomes unsaturated. While the point at which increase in suction is associated by reduction in water is referred to as residual point. These breaking point are divided into three zones; transition, residual and boundary effect zone (Fredlund, 2012).

There have been several tests procedures developed to improve SWCC due to its significant. In order to achieve a good fitting for experimental data in SWCC, mathematical models were developed. The first suction measurement was used in Europe (1920's) and introduced in the United States by Gardner in 1937 using a filter paper method. This paper method is quite simple and inexpensive. It is known as the only method for measuring the full range of soil suction as well as measure the matric and total suction concurrently. Fredlund, (1993) states that the filter paper method assumes it will reach equilibrium with respect to the moisture flow within the soil.

Many researchers used the filter paper method by implementing different method (McKeen 1980; Chandler & Swarbrick, 1995).

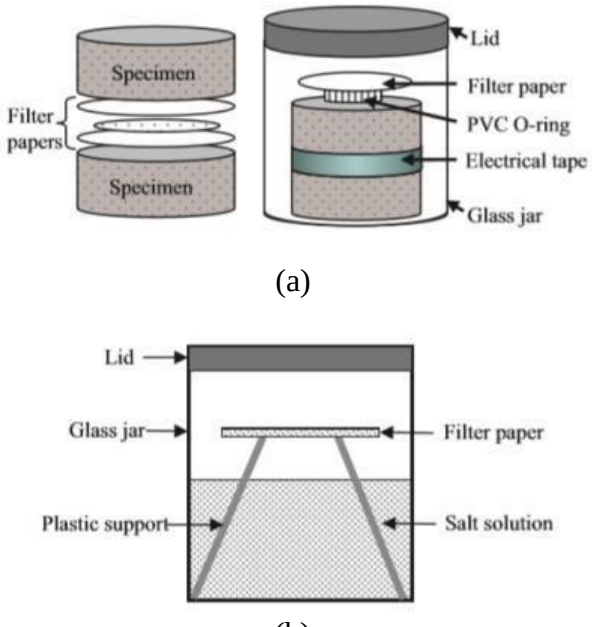

Figure 2.8: Filter Paper Configuration: (a) Soil Suction Measurement by Filter Paper (b) Filter Paper Calibration (Yang, 2015)

The diagrammatic representation of measuring soil suction and filter paper calibration method is shown in Figure 2.8. Determination of matric suction of a soil requires three filter papers. They were placed in contact with the soil. The middle filter paper is

generally used as matric suction measurement, while the other two filter paper serves as protection from contacting the soil. The precision of matric suction is dependent on the good contact of filter paper with the soil sample and maintenance of temperature. The types of filter paper for suction measurement includes; Schuell No. 589 White Ribbon, Whatman No. 42, Schleicher and Fisherbrand 9-790A, as recommended by ASTM D 5298. The most common filter paper used is Whatman No. 42, ash-free quantitative Type having 5.5cm diameter. In using sodium chloride salt solutions, the curve obtained for Schleicher & Schuell No. 589- WH filter papers is shown in Figure 2.9.

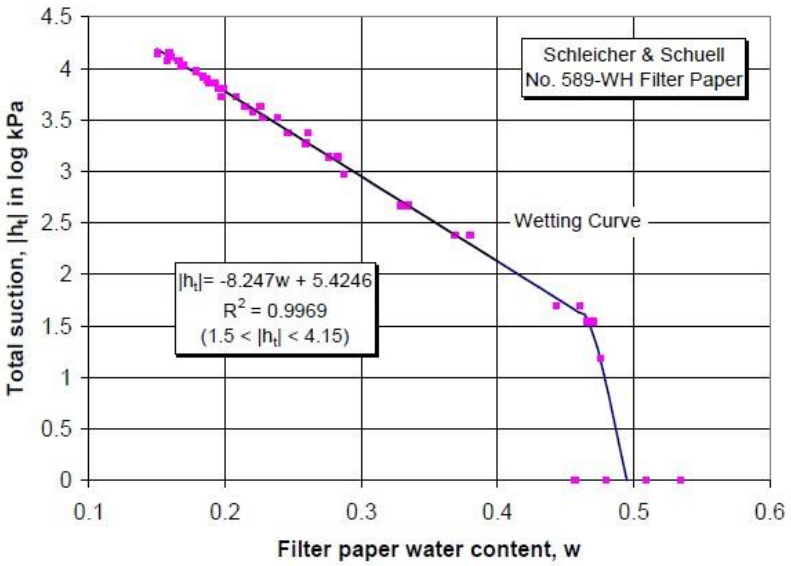

Figure 2.9: Filter Paper Wetting Calibration Curve (Bulut, 2001)

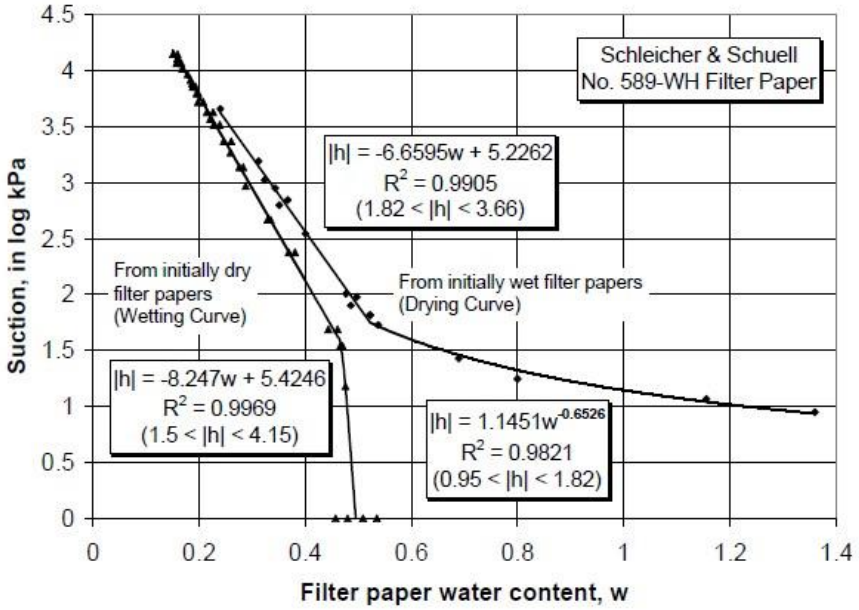

Figure 2.10: Matric and Osmotic Suction Calibration Curve (Bulut, 2001)

In Figure 2.10, the drying curve was established from filter paper test results. The pressure membrane and pressure plate is used to obtain curves for Schleicher & Schuell No. 589-WH filter papers. The data point as seen in Figure 2.10 represent an average of three tests and each of the test is an average of about four filter papers.

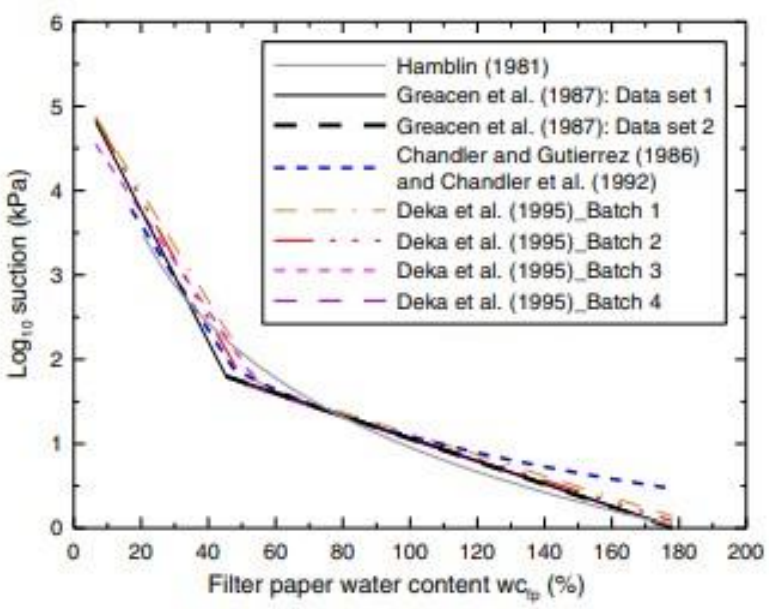

Figure 2.11: Comparison of Calibration Curves (Kim, 2016)

From all the calibration curves shown in Figure 2.12, ASTM D5298-10 agreed with the proposed equations of Greacen et al. (1987). It was developed by the original data presented by Fawcett and Collis George (1967).

Chapter 3

METHODOLOGY

3.1 Introduction

The testing procedures and approaches employed to examine the desiccation cracks on soil specimen were studied and described in this chapter. All laboratory testing were performed according to the American Standards for Testing and Materials (ASTM) and British standards.

3.2 Material

3.2.1 Soil Sampling

The soil sample used for this research was collected from a site behind Marmara dormitory beside Eastern Mediterranean University mosque. A trackhoe excavator was used to enable undisturbed sampling below a depth of approximately 1.5 m from the ground surface.

Figure 3.2 shows the soil sampling and the samples taken from the selected location. The approximate coordinates of the selected location are (35°08'50.6"N, 33°54'13.2"E) as seen in Figure 3.1. Table 1.1 shows the physical properties of the soil samples used in this study.

Figure 3.1: Site Location, Google Map.

(a) (b)

Figure 3.2: Soil Sampling, (a) Depth of Soil Sample (b) Soil Samples Placed in Buckets

Table 1.1: Physical Properties of the soil used in study

Physical Properties	Values
Liquid limit, LL (%)	62
Plastic limit, PL (%)	31
Plasticity Index, PI (%)	31
Linear shrinkage (%)	18
Specific gravity, G_s	2.68
pH	8.07
Specific surface area (m^2/g)	143
Clay size fraction (%)	56.8
Silt size fraction (%)	43.0
Sand size fraction (%)	0.2
Fines fraction (%)	99.8
Insitu dry density (g/cm^3)	1.3
Insitu water content, w (%)	29.8
Unified Soil Classification System	CH

In the above obtained results, the soil was found to be an inorganic clay and according to the unified soil classification system, it was classified as highly plastic clay, CH.

3.3 Testing Strategy

In order to study the clay behavior of desiccation cracks, a testing strategy is designed. The testing program is divided into four main groups; in the first and the second testing group, the clay samples were prepared at initial moisture content above the liquid limit in order to observe and analyze the cracks due to drying. Whereas in the third and fourth testing group, the tensile strength was carried out using the double punch test and the matric suction of clay specimens were measured.

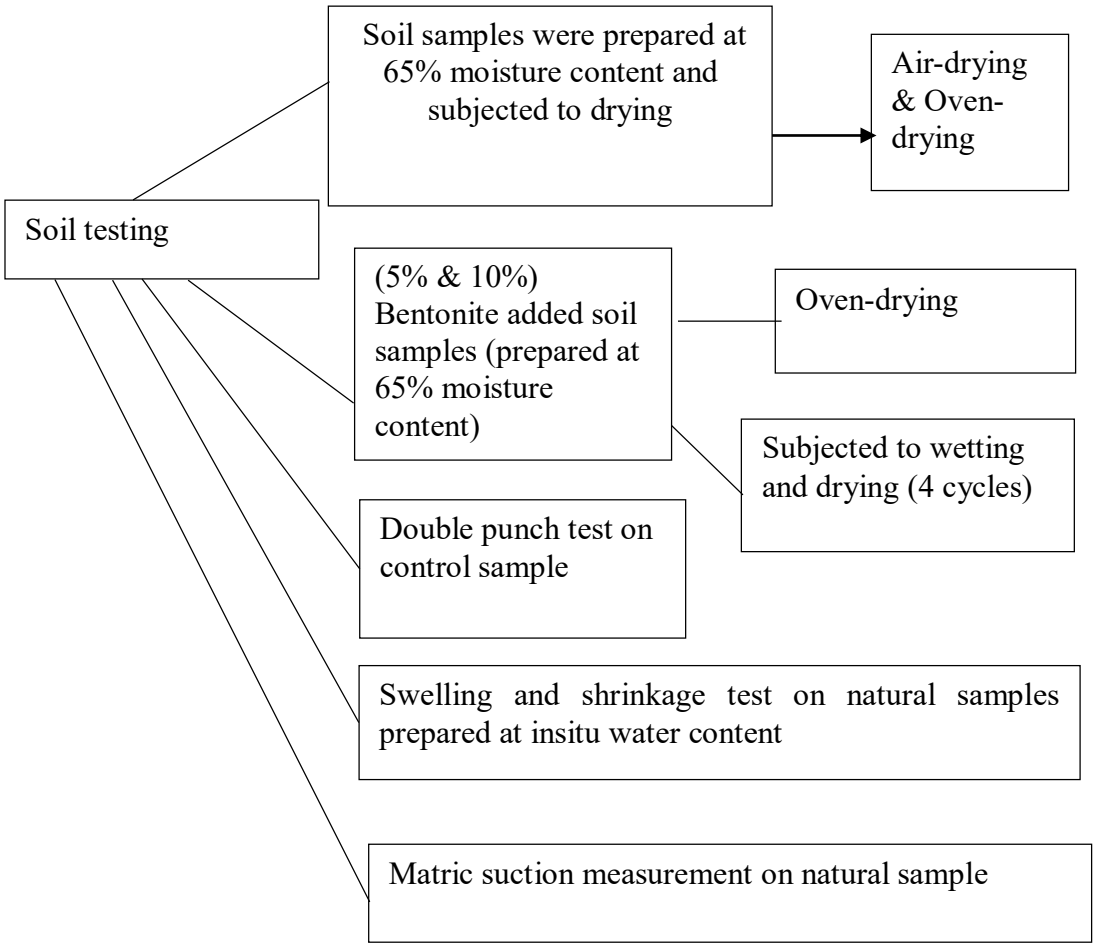

Figure 3.3: Testing Strategy of Soil Sample

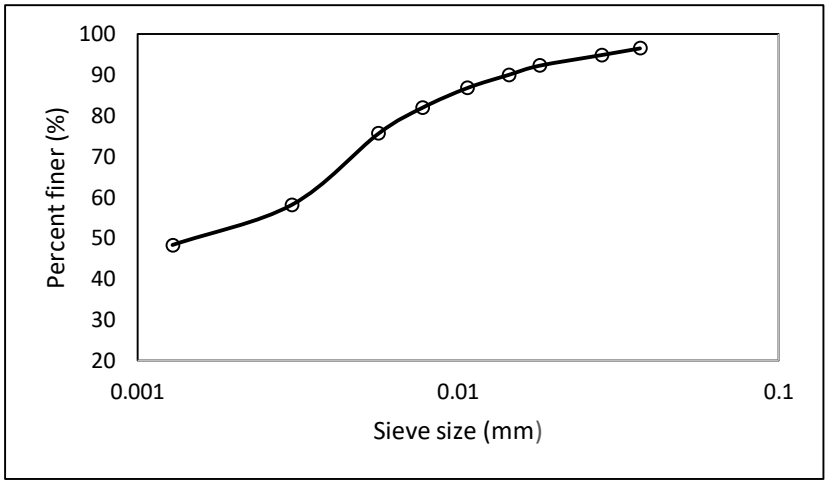

Figure 3.4: Particle Size Distribution Curve of the Soil Specimen used in the Study

3.3.3 Atterberg Limits

The liquid limit of the soil sample was determined according to ASTM D4318 test standard (Figure 3.5). In the determination of plastic limit of soil sample, ASTM D4318 test standard was followed. Following the ASTM standard test procedure, the obtained test results for liquid limit and plastic limit were 62% and 31% respectively as given in Table 1.1.

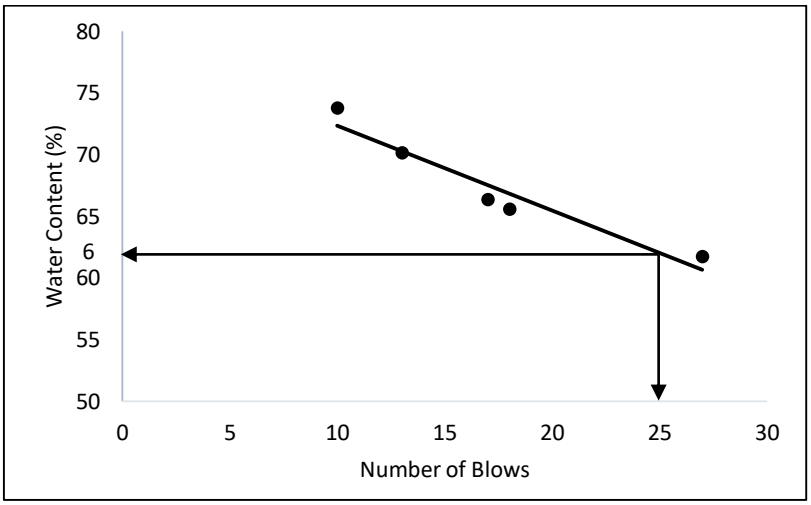

Figure 3.5: Liquid Limit Test Result

3.3.4 Linear Shrinkage

This is the reduction in length of soil specimen when oven-dried with moisture content at the liquid limit. The soil sample passed through sieve number 40. The test was determined by applying BS 1377 test procedures. By following the test procedures, the linear shrinkage of the soil was found to be 18%.

3.3.6 Specific Surface Area

This refers to the ratio of surface area to unit mass. This soil property is performed according to Ethylene Glycol Monoethyl Ether (EGME) test procedures suggested by Cerato & Lutenegger, (2002).

In the test, 1g of oven-dried soil sample having passed through sieve number 40 is placed in an aluminum tare. The mass of the soil is determined to the nearest 0.0001g. Thereafter, using a small pipette to measure 3ml of Ethylene Glycol Monoethyl Ether (EGME) is placed gently over the soil. Then the soil is gently mixed thoroughly until the mixture forms slurry and appears uniform. The tare is placed into a vacuum desiccator with a small plexiglass lid over the tare at 2 – 3 mm apart. The sample is then left for 10hrs to determine the mass of soil mixture. Then the process is repeated at approximately 18hrs and at 24hrs and the weight of soil mixture is measured not varying more than 0.0001g. The specific surface area (SSA) of the tested soil was determined to be $143 m^2/g$.

3.3.7 Matric Suction

This is used to determine the relationship between moisture content and suction. The test is performed following the ASTM D5298 standards. For this study, determination of the matric suction was performed. Firstly, Whatman No. 42 type filter papers to be used is dried in the $105 \pm 5^{o}C$ temperature oven for 16hr and afterwards kept in a

desiccator to cool. The soil sample was prepared and placed in a plastic bag for 48hrs in order to be uniform. The soil sample were then placed in the specimen container and cut into half with three filter papers in contact with the soil. The filter paper in the middle is used to measure the matric suction while the other two are used to prevent the filter paper in the middle from soil contamination. The two half samples were taped together, thereafter the soil specimen were placed in a glass jar and sealed in a well-insulated container for suction equilibium. It was allowed for 14days before taking the soil specimen, specimen containers and filter papers out of the insulated container for weighing. Figure 3.6 and 3.7 shows the specimen carried out for this test.

Figure 3.6 Measurement of Matric Suction

Figure 3.7: Soil Specimen Placed in a Jar

3.4 Preparation of Soil Samples of Measuring Desiccation Cracks

The test for the measurement of desiccation cracks were prepared according to Priyankara, (2016). The soil samples were oven dried at 60^{o}C and pulverized by using the grinding machine. Then the soil samples were mixed with water at an initial water content (65%) slightly above the liquid limit of the soil. The mixed soil samples were placed in plastic bags so that homogeneous soil-water mixture was obtained. Ten number of circular desiccation molds with 50 cm diameter and 19 cm height were prepared. The bases of the circular molds were grooved to prevent the soil from sliding.

Thereafter, mixed soil samples were carefully placed into the molds by tamping the molds gently so that no trapped air remained within the soil layers. The soil specimens were prepared at 65% water content in order to observe the crack propagation as well as the shrinkage curve. The prepared soil specimen was subjected to air-drying under room temperature and also to oven drying at 60^{o}C. The water content of soil specimen in each desiccation mold was determined at different time intervals.

In the same vein, four soil specimens were prepared. The first two specimens were prepared by the addition of 5% and 10% bentonite. They were subjected to an oven-drying condition at 60^{o}C. The rate of drying was measured hourly up to 7hrs, then after 24hrs and finally 48hrs thereafter. The water content of specimen, void ratio was determined at different timings.

In the case of wetting-drying cycles, the other two prepared specimen containing 5% and 10% bentonite respectively were subjected to the same desiccation method. Firstly, the weight of wet specimen was measured and placed in the oven for 48hrs. The estimated loss was determined and a measure of water was added back. The specimens were gradually saturated using a wash bottle and continues till the mass loss is recovered. After completing the wetting cycle, they were wrapped with membrane to prevent evaporation. Thereafter specimen was left for 24hrs so as to take in water back to its initial state. At this point, the wetting cycle ends and the second drying cycles begins with specimen subjected to oven drying. At the end of every cycle, images were captured for analysis using imageJ software.

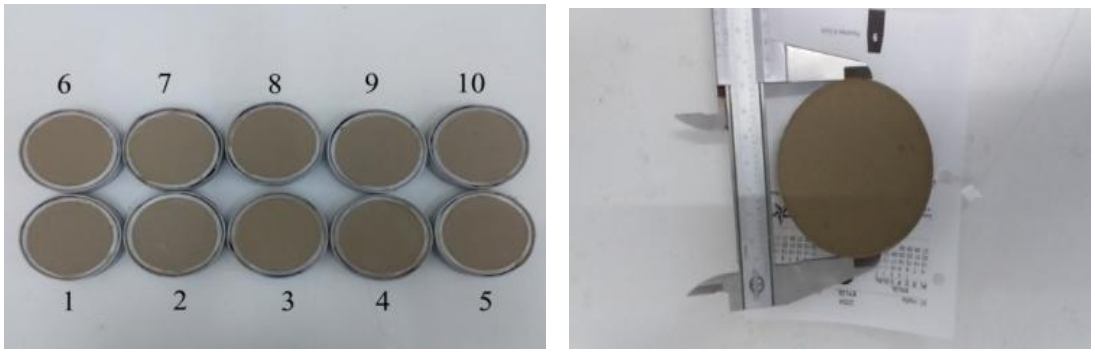

(a) (b)

Figure 3.8: (a) Prepared Soil Specimen for Desiccation Cracks (b) Dimension of the Soil Specimen

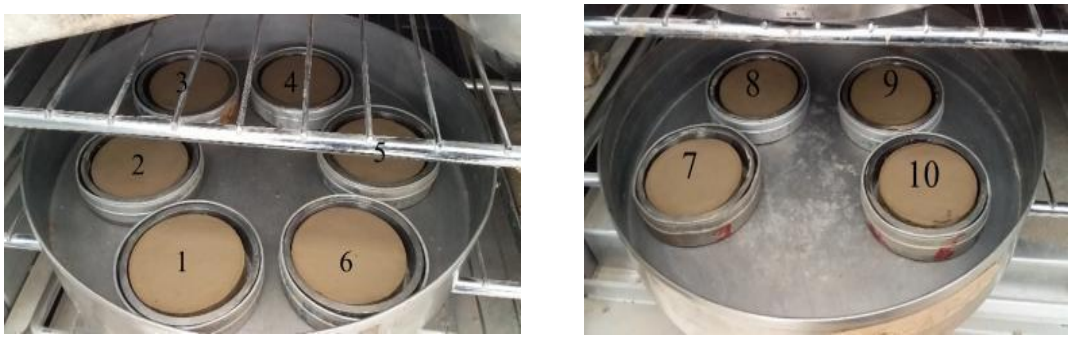

Figure 3.9: Soil Specimen for Desiccation Cracks During Oven-drying

(a) (b)

Figure 3.10: Bentonite Added Soil Specimens (a) in the Oven (b) After wetting

3.5 Double Punch Test

This test method was proposed by Chen (1972) and described by the use of two punch discs placed at the center of a cylindrical specimen on the top and bottom surfaces.

The load is applied on the discs until the specimens fails. For this study, the soil sample was compacted with an in situ dry density and insitu water content as given in Table 1.1. The specimen was cured for 2 days and were tested. The diameter of steel spacer discs was 38mm as recommended by Kim et al. (2007). The load is applied vertically such that the top and bottom metal discs are placed at the center of specimen. The top and bottom caps produced from Teflon material is used to reduce measurement error and also to keep weight light having holes at the centers having metal discs of same size. During the test, the caps were well connected with tiny springs in order to minimize external pressure on the sample (Chen,1972).

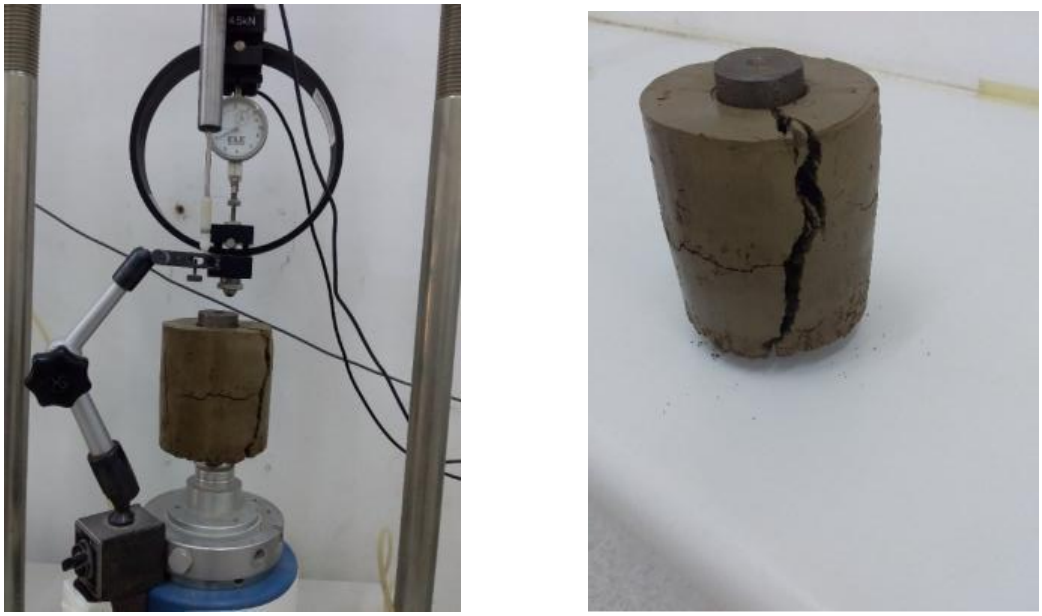

(a) (b)

Figure 3.11: (a) Experimental Test Set-up (b) Failed Soil Specimen

3.6 Swelling and Shrinkage Potential

The soil specimen was prepared with the insitu water content and insitu bulk density. The soil-water mixture was cured for 48hrs by keeping it in a plastic bag. This allowed water to distribute uniformly throughout the soil mass. The test was conducted using a conventional odeometer in a free swell. The specimen was inundated and allowed to

swell. It took about 3 days to complete its swelling. The specimen was taken out after the completion of swelling and placed in the desiccator to undergo shrinkage using silica gel. The specimen was measured at different time intervals in order to determine its water content and void ratio. The drying process was gradual and it was achieved under room temperature.

(a) (b)

Figure 3.12: (a) Swell Test Set-up (b) Drying Specimen in a Desiccator

3.7 Image Processing

The extraction of significant data from digital image is carried out by means of an image processing called image analysis. This is performed in two stages. The first stage is the stage in which image is prepared for analysis. It involves the conversion of Red Green Blue (RGB) image from camera to grey scale and then the binary image obtained after threshold of grey scale image. The second stage is the analysis of the processed image that has been obtained in order to calculate parameters characterized by cracks such as crack intensity factor. Figure 3.13 shows the flow diagram of an image processing for ImageJ software.

1. Prepared Raw Image

Images are captured with the aid of camera in RGB (Red Green Blue). An imageJ software with a cropping circular tool used to crop the area. This involve selecting the circular area of mould and crop the outer area in order to achieve RGB image having a white background. Thereafter the image is converted to grey scale image of 8-bit (Tiwari, 2015). This can be done by selecting the option; Image type 8-bit on the ImageJ window.

2. Grey-Scale Processing

This is performed to aid correction. Two operations are carried out: by removing continuous backgrounds and sharpen edges of image (Tiwari, 2015).

3. Image Segmentation

This is performed to isolate shrinkage and crack area from the soil specimen. The grey scale image is threshold at a fixed value. It can be done by selecting the option Image-adjust-threshold in the window image. The threshold value can be corrected manually if the value is not given. It divides the image to several regions. (Tiwari, 2015).

4. Binary Processing

If there be any error on the image like shrinkage and crack area after segmentation, then a binary operation can be used to correct the basic error ((Tiwari, 2015).

5. Image Analysis

The processed image having undergone binary operations is finally analyzed.

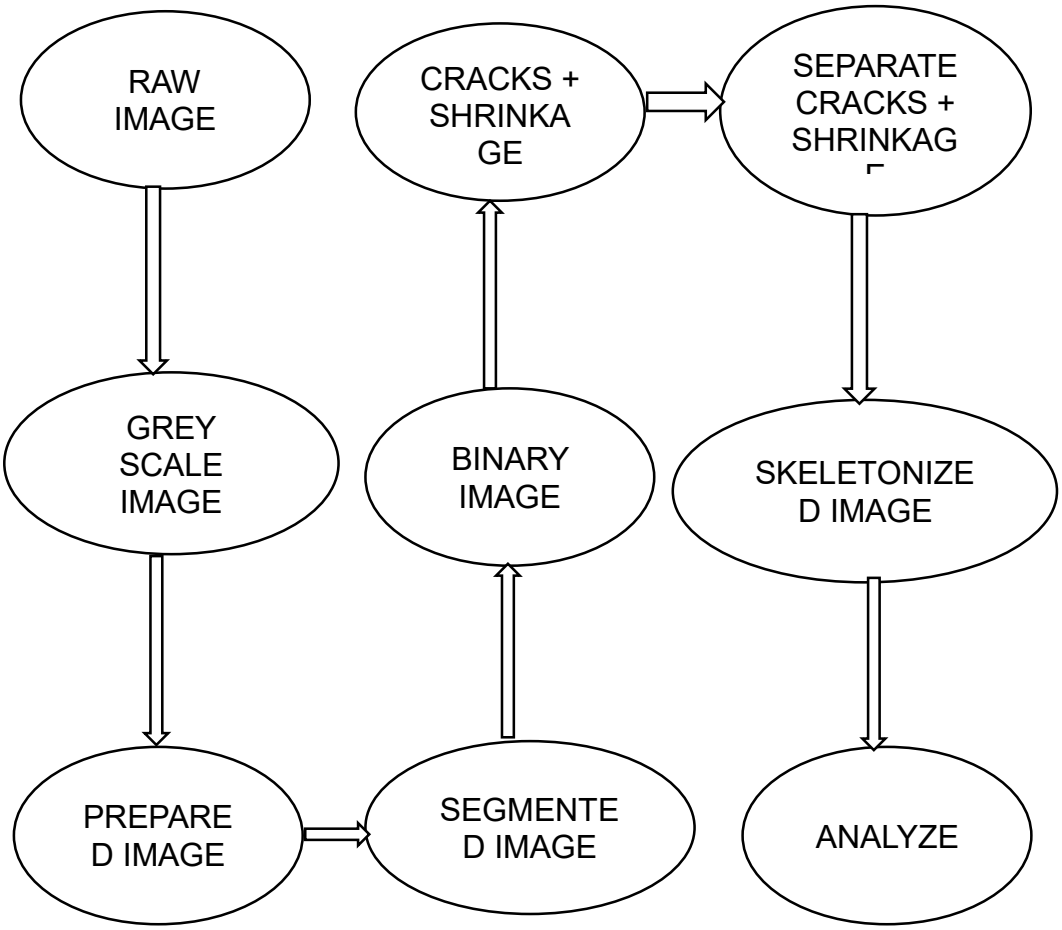

Figure 3.13: Flow Diagram of Image Processing (Tiwari, 2015)

Chapter 4

RESULTS AND DISCUSSION

4.1 Introduction

In this chapter, the experimental results for desiccation cracks, tensile strength, wetting – drying cycles, swelling and shrinkage as well as the matric suction of the specimens are presented. The results are compared with previous studies.

4.2 Soil Behaviour at Air-drying and Oven-drying Conditions

The volume change of the soil specimen being prepared were observed with respect to time. The soil specimen has the same initial moisture content of 65%, slightly above the liquid limit of the soil. It can be seen in Figure 4.1 and Figure 4.2 that the water content gradually decreases with time. As the constant evaporation stage which is the first stage of drying ends, the air entry value (AEV) is attained. At this point, air begins to enter into the pore spaces of the soil due to increase in suction. As a result of this, the soil transit from saturated to an unsaturated form. The duration to attain the AEV when specimen was subjected to oven-dry was lower at (30 hrs) in comparism to air-dry (200 hrs) due to the rapid rate of desiccation in oven drying. In Figure 4.1, the falling evaporation stage began below 9% water content representing the AEV and in Figure 4.2 the falling evaporation stage began around 12 % water content and the AEV can be seen in the figure.

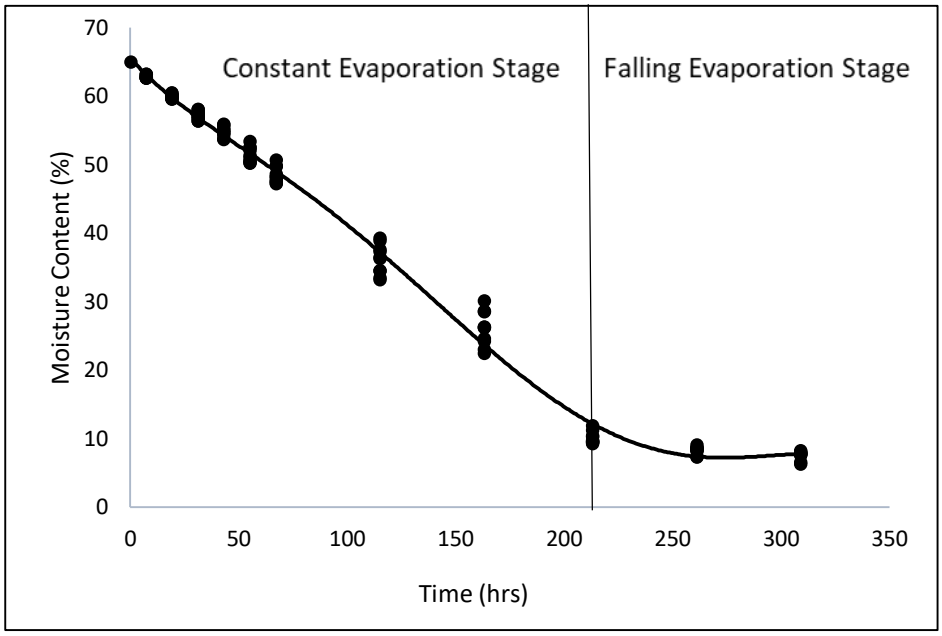

Figure 4.1: Oven- drying of Natural Soil Specimen

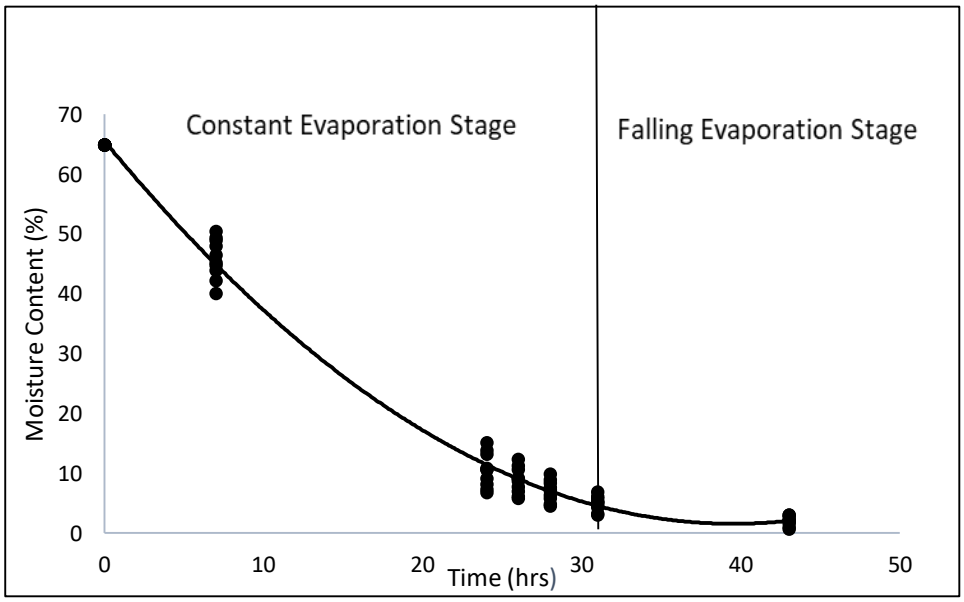

Figure 4.2: Air-drying of Natural Soil Specimen

In order to observe crack development and crack pattern, 10 specimen having the same initial moisture content were prepared. In Figure 4.3, it can be seen that cracks did not occur due to slow rate of drying in air drying conditions whereas for oven dried specimens in Figure 4.4 cracks were observed at the 8^{th}, 9^{th} and 10^{th} specimen having

water content below 10%. This occurred due to the gradual increase in the soil porosity because of the evaporation of some trapped moisture in soil micro pores and resulted in the cracking of the soil specimens.

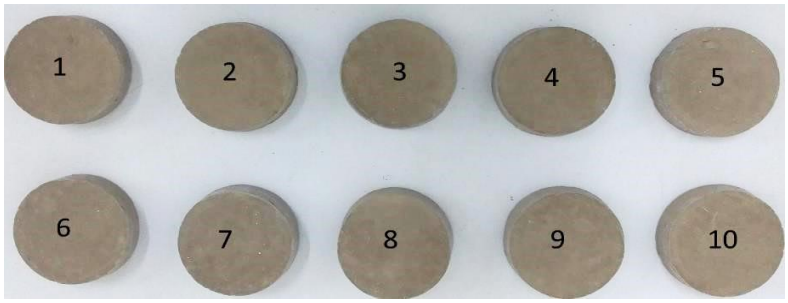

Figure 4.3: Clay Specimen After Air-drying

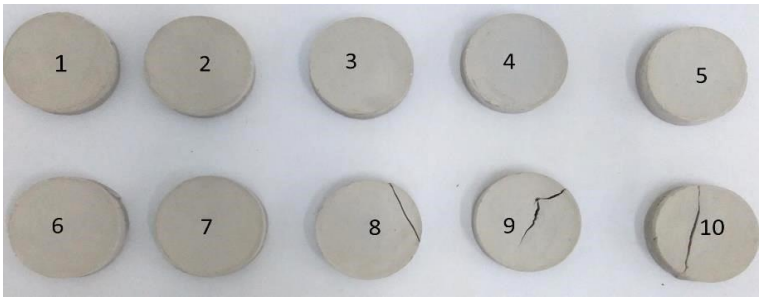

Figure 4.4: Clay Specimen After Oven-drying

4.3 Volume Change Behavior of Natural Soil

A, S-shaped curve was suggested by Hanafy (1991) in describing the volume change for an expansive clay soil, by a change in void ratio in relation to change in water content. The curve starts with an initial structural shrinkage followed by a decline during normal shrinkage and decreases during residual shrinkage according to Haines (1923). The curves in Figure 4.5 have almost similar trend in soil behavior.

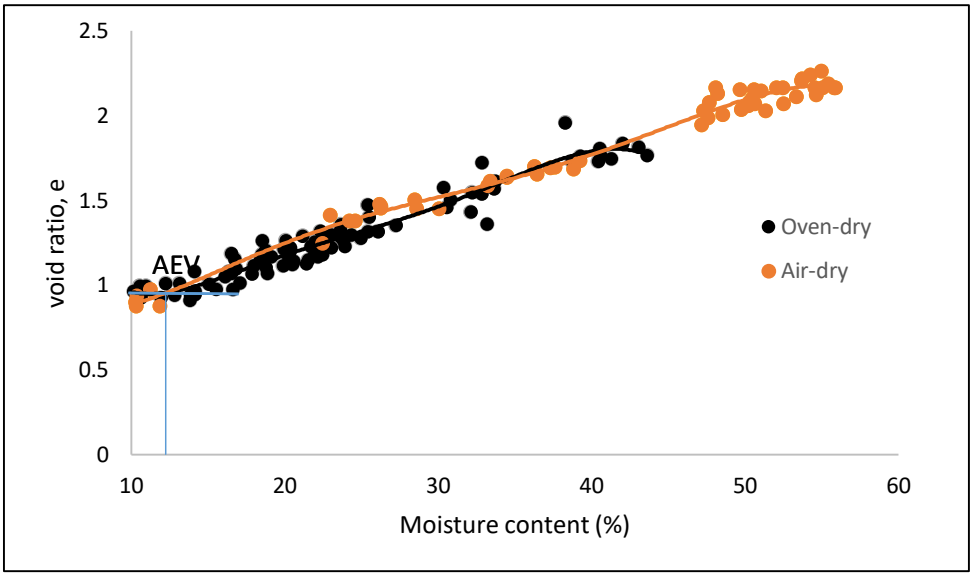

Figure 4.5: Shrinkage Curves of Oven-drying and Air-drying Specimen

4.4 Behavior of Bentonite Added Soils using Oven Drying

Soil samples containing 5% and 10% bentonite were subjected to oven-drying. This was performed in order to observe the cracks developed in the bentonite added specimens. The specimens were oven-dried at a temperature of 60ºC. In Figure 4.6, it is observed that there was no significant crack development during and after the oven drying process.

Figure 4.6: Soil Specimen with 5% and 10% Bentonite After Oven-drying

The desiccation curves of the oven-dried specimen in Figure 4.7, show two distinct evaporation stages. The period where moisture content decreases with time is referred to as constant evaporation. While the period where moisture loss decreases steadily until residual water content is achieved is referred to as falling evaporation. Both stages were carried out for 48 hours. In Figure 4.7 and Figure 4.8, the residual water content for 5% and 10% bentonite is about 3% and 4% respectively. The same trend of desiccation curve was observed with the control specimen under the air-dried and oven-dried conditions. The moisture content decreases linearly with time before gradually reaching its residual moisture content. From the figures, no significant change was evident with increase in bentonite content but when subjected to wetting and drying process, significant change was noticed.

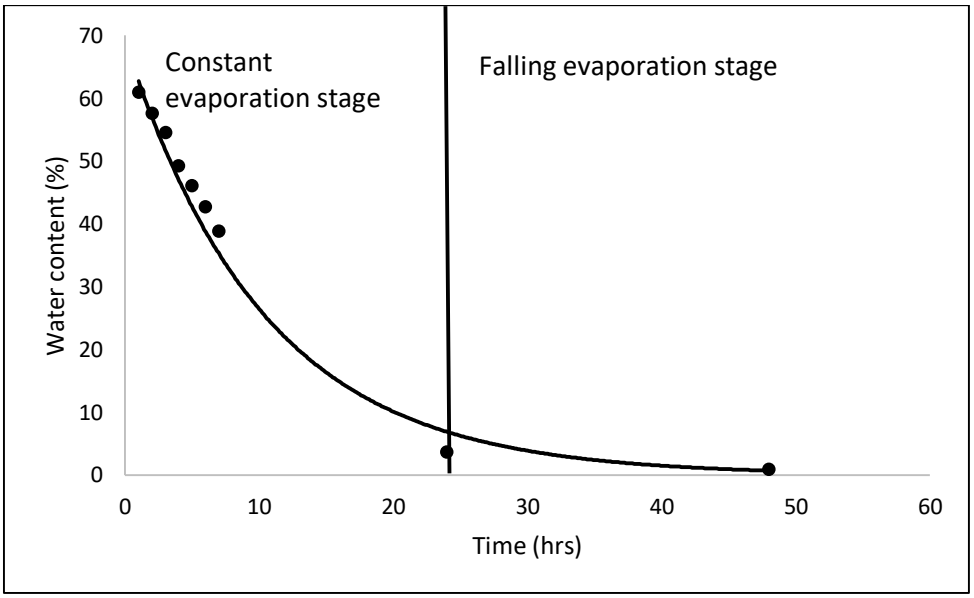

Figure 4.7: Desiccation Curves of 5% Bentonite Added Soil Specimen

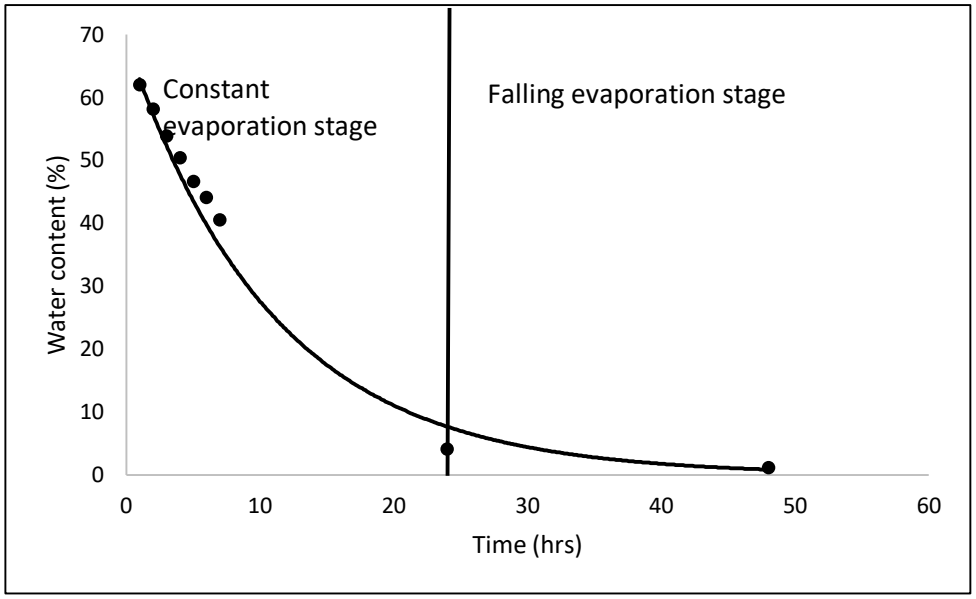

Figure 4.8: Desiccation Curves of10% Bentonite Added Soil Specimen

4.5 Volume Change Behavior of Bentonite Added Soil Specimen

In comparison with the control specimen under air and oven drying conditions, the change of void ratio with respect to time is similar when 5% and 10% Bentonite was added to the clay specimen. There were no cracks observed in the process even at its residual state. The results are shown in Figure 4.9.

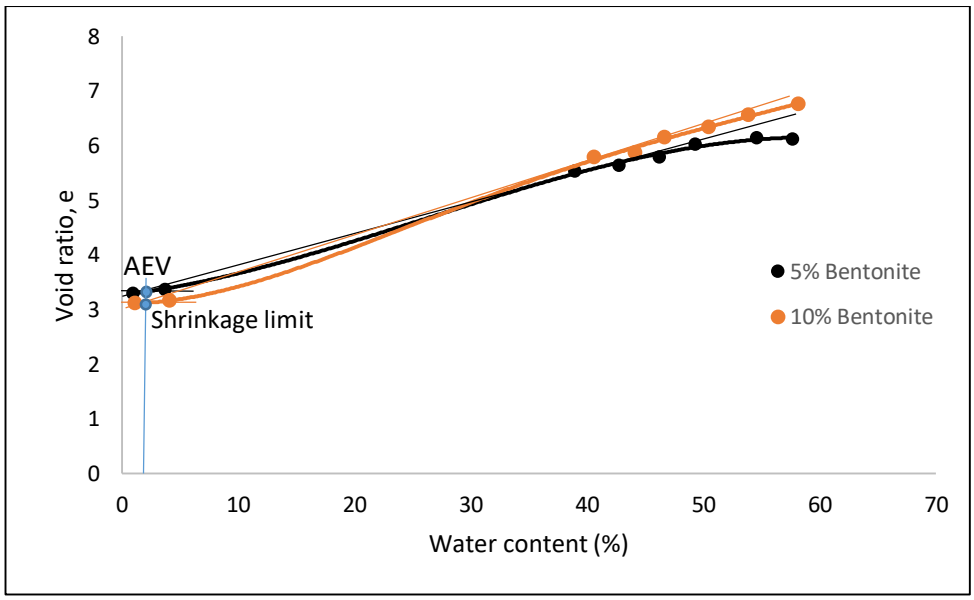

Figure 4.9: Change in Void Ratio Versus Water Content of 5% and 10% Bentonite Added Soil Specimen

4.6 Crack Pattern of Bentonite Added Soils under Wetting-drying Cycles

In the present study, the prepared bentonite added soil specimen were dried at 60ºC temperature in the oven and the specimens were subjected to wetting-drying cycles. Subsequent cycles were compared by visual observation at the end of each cycle. During the cyclic testing, it was observed that several factors influenced the crack initiation and pattern. This includes; sample preparation procedures, surface imperfections and soil texture. They had significant impact on the crack geometry, crack pattern, repeatable cycles and crack intensity factor, CIF. In the same way, plasticity of soil and mineral composition reveals the behavior of crack geometry and crack propagation. Following the laboratory investigations, Figure 4.10 and Figure 4.11 shows the variation of crack intensity factor, CIF versus number of cycles. The CIF was calculated by using the equation given below:

$$\text{CIF} = \frac{\text{Cracked area}}{\text{Specimen Area}} \text{ x } 100 \qquad (5)$$

In order to measure the amount of cracking, crack intensity factor is calculated by determining the percentage of surface area of cracks to total surface area of specimen. Crack images were analyzed using ImageJ software. It can be seen in Figure 4.10 that the CIF increased continuously to the third cycle and a slight increase after this cycle. In Figure 4.11, the CIF increased steadily per number of cycles. Each cycle is achieved after completion of wetting-drying. The presence of bentonite in the soil specimen increased the activity of the soil specimen and resulted in crack development.

As it can be seen in Figures 4.12, 4.13, 4.14 and 4.15 the cracks were created from the middle of specimen. These findings are in good harmony with the findings of Avila et al., (2013); and Nahlawi & Kodikara, (2006).

Costa et al. (2013) proved that the development of tensile stress which result into tensile failure has to do with clay fraction. These are the governing issues in crack initiation and propagation. In Figures 4.10 and Figure 4.11 the intensity of crack was significant as the crack intensity factor increases with increasing bentonite content and cycles. This is as a result of attraction of bentonite to water, thus reducing desiccation rate and eventually cracking occurs.

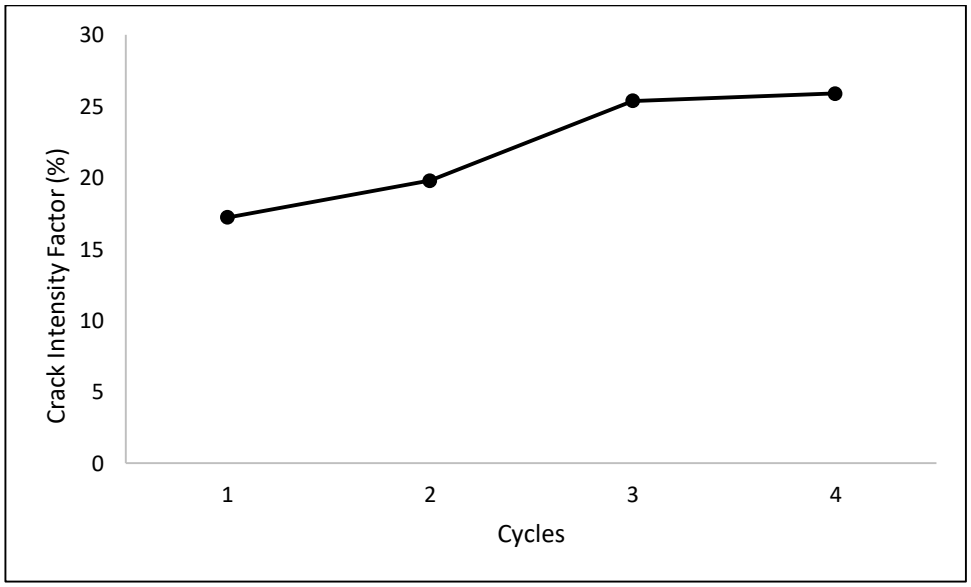

Figure 4.10: CIF Versus Number of Crack Cycles (5% Bentonite)

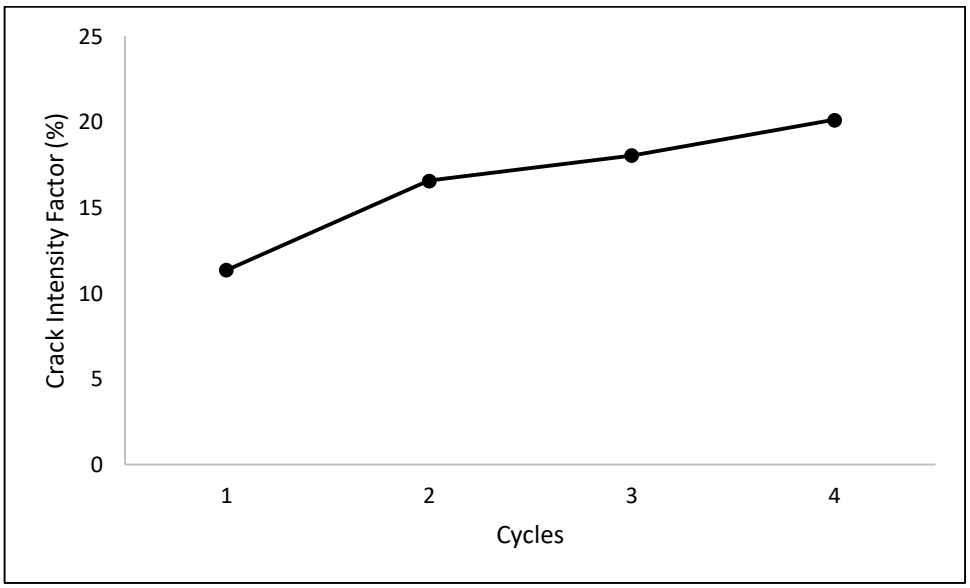

Figure 4.11: CIF Versus Number of Crack Cycles (10% Bentonite)

The specimen in Figure 4.12, 4.13, 4.14 and Figure 4.15 show the horizontal and the vertical cracks. The desiccation method employed is an oven-dried condition. As the drying rate continues, the tensile stress in soil increases. This reduces the soil strength and consequently cracks are formed.

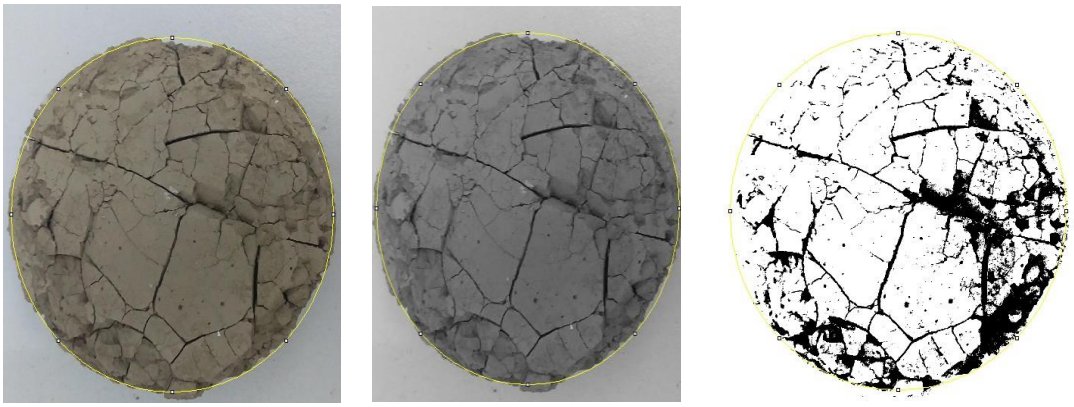

(a) (b) (c)

Figure 4.12: 5% Bentonite Added Soil Specimen After 1st Cycle (a) Raw Image (b) Grey Scale Image (c) Threshold image

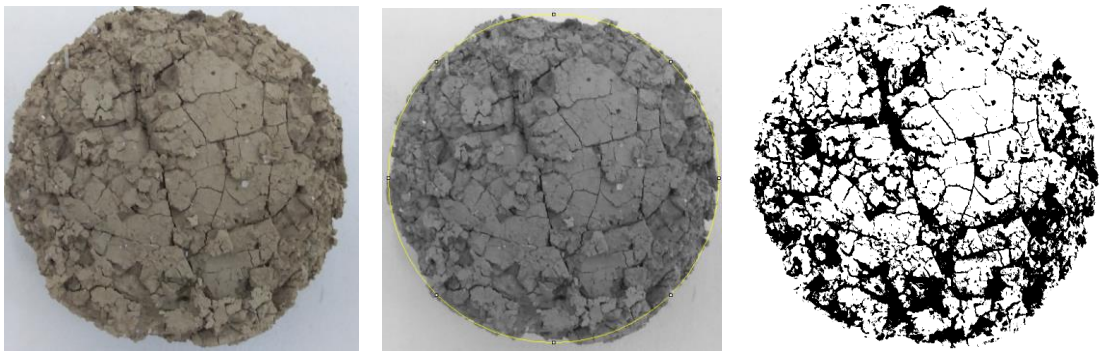

(a) (b) (c)

Figure 4.13: 5% Bentonite Added Soil Specimen After 2nd Cycle (a) Raw Image (b) Grey Scale Image (c) Threshold Image

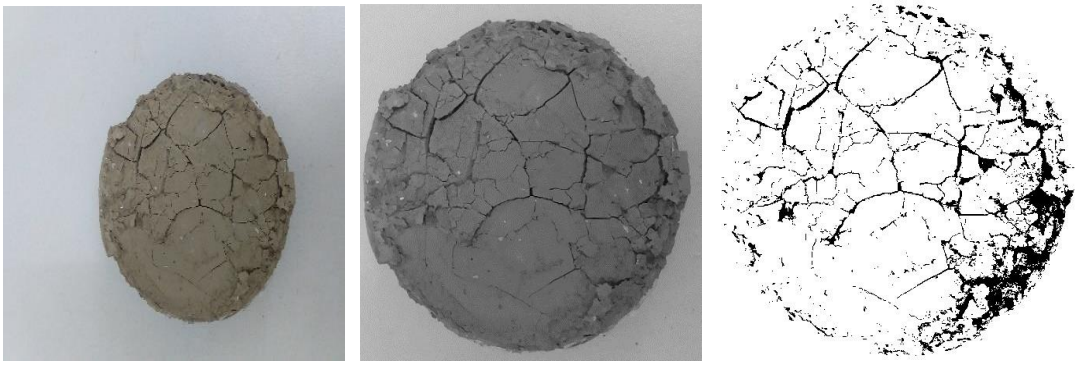

(a) (b) (c)

Figure 4.14:10% Bentonite Added Soil Specimen After 1st Cycle (a) Raw Image (b) Grey Scale Image (c) Threshold Image.

(a) (b) (c)

Figure 4.15: 10% Bentonite Added Soil Specimen After 2nd Cycle (a) Raw Image (b) Grey Scale Image (c) Threshold Image.

4.7 Tensile Strength of Natural Soil: Double Punch Test

The tensile strength of soil is significant especially in the design of slopes, highway embankments and other earth structures where tensile cracks cause erosion and landslides (Ge and Yang, 2013). In the study, the tensile strength of the natural soil was determined according to the test procedure as proposed by Fang and Chen 1971.

(a) (b)

Figure 4:16:Double Punch Test: (a) Sample After Failure (b) Radial Tension Cracks

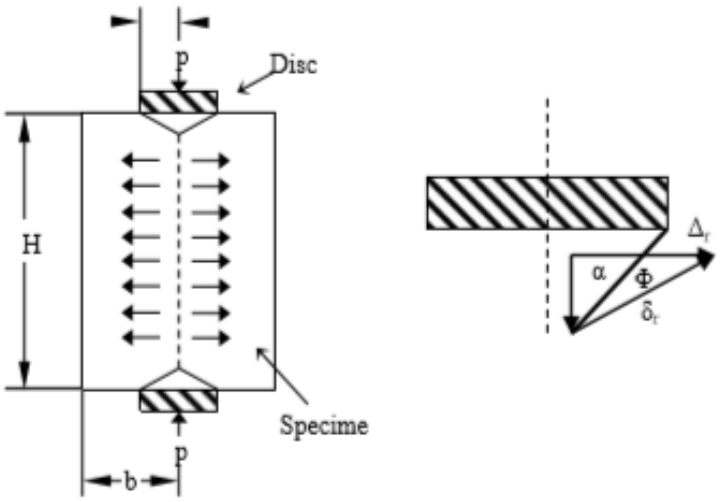

(a) (b)

Figure 4.17: Diagrammatic Representation of Double Punch Test (Chen, 1972)

Figure 4.16 illustrates an ideal failed mechanism for a double punch test using a cylindrical compacted specimen. It comprises of small tension cracks that corresponds to the radial direction. Figure 4.17 shows the sample after failure in double punch test and the radial tension cracks. The double punch test was performed on the natural soil and the obtained test results were shown in Figure 4.18. The figure shows the axial force applied on the cylindrical test specimen and the corresponding axial displacement values.

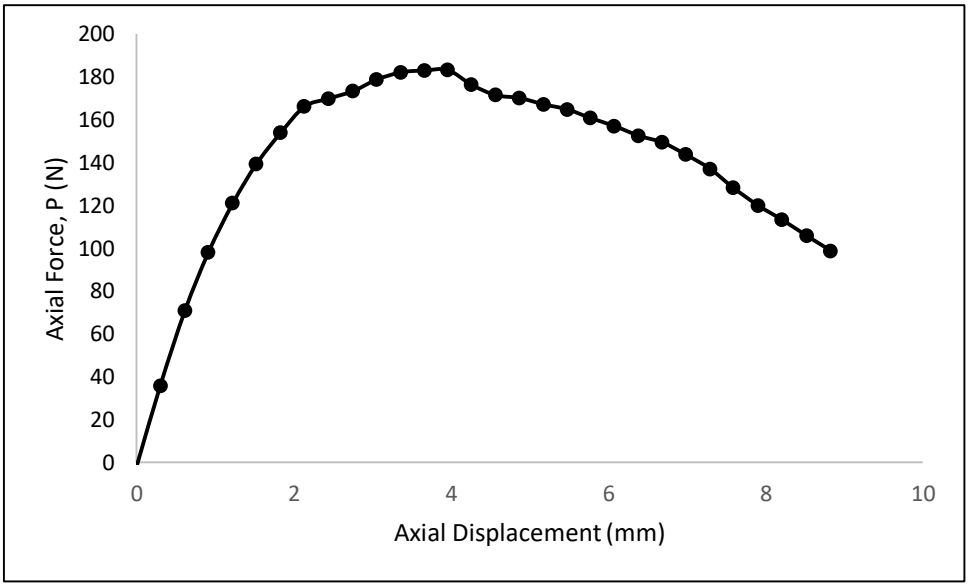

Figure 4.18: Double Punch Test Result of Natural Soil

According to the double punch test results in Figure 4.18, the maximum tensile strength of the natural soil was obtained under the applied axial force of 180 N.

4.8 Swelling and Shrinkage Test for Natural Soil

Figure 4.18 shows the free swelling versus time of the natural soil. The values given on the y-axis are the percentage change in the height of soil specimens. It can be seen that an increase in swelling as a function of time was gradual at the starting point, then increased suddenly and thereafter it reached asymptotic value. That could be explained due to the time needed for water to reach the micro pores of the specimen and cause swelling. Figure 4.20 and Figure 4.21 depicts the shrinkage of the samples as the diametric and volumetric strain decreased slightly with respect to time.

The water content and void ratio decline slightly and reached equilibrium as presented in Figure 4.22.

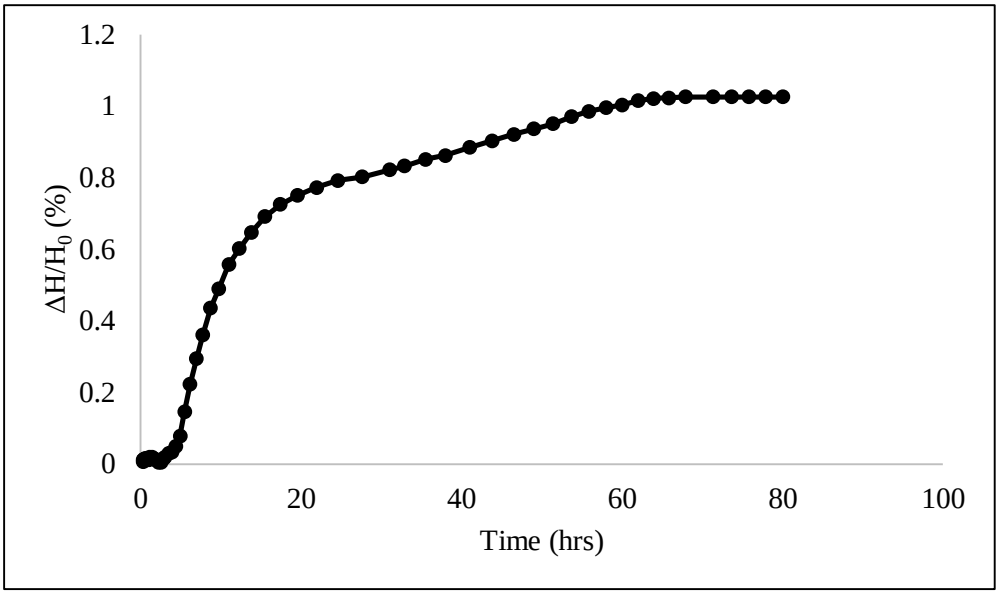

Figure 4.19: Swelling Behavior of Natural Soil

Figure 4.20 and Figure 4.21 represent the diametric and volumetric strain versus time, respectively. A decrease in volume of the soil is due to evaporation of moisture that exist in its soil pores. While drying the soil, capillary tension appears leading to cracks in soil. Figure 4.20 and Figure 4.21 indicate that as water evaporates from soil pores, the volume changes in the soil become stable with time and no further changes in volume occur with time.

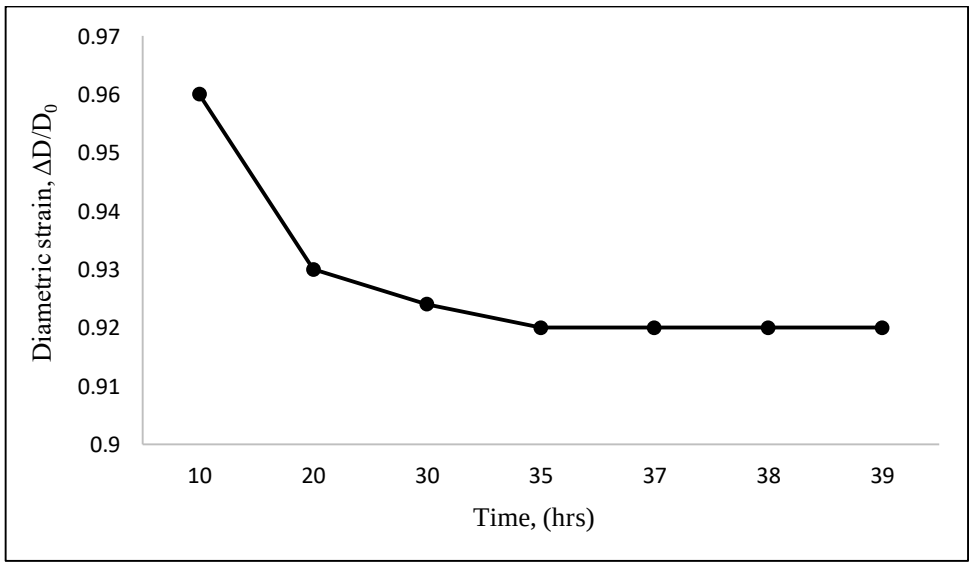

Figure 4.20: Diametric Strain Versus Time

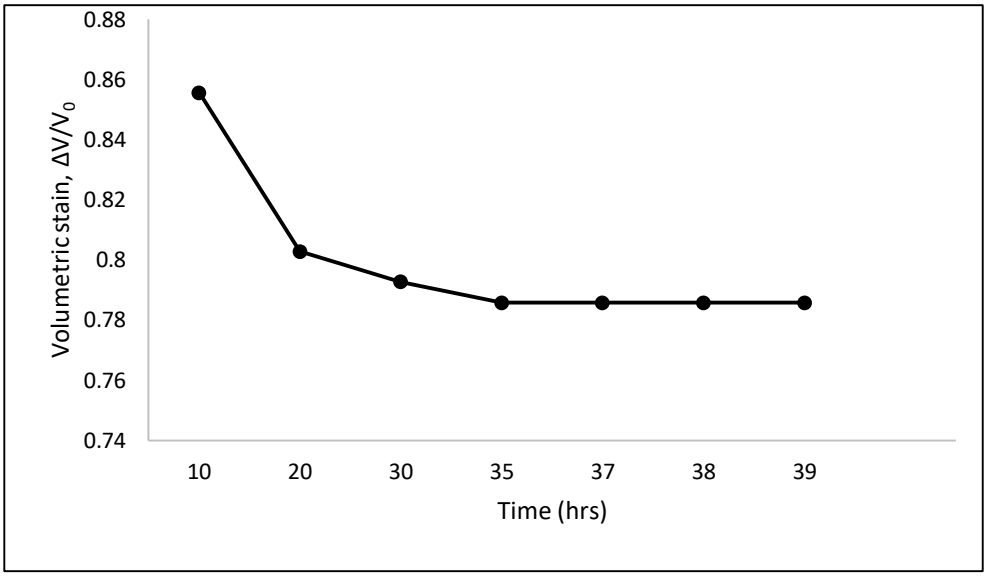

Figure 4.21: Volumetric Strain Versus Time

The values in Figure 4.21 were obtained by subjecting the natural soil specimens to drying with the use of silica gel in a desiccator. From Figure 4.21, the air entry value, AEV of the specimen was found to be at a water content below 34%. At this point, air begins to enter into the soil pores due to increase of suction. As a result, soil transit from saturated to an unsaturated state.

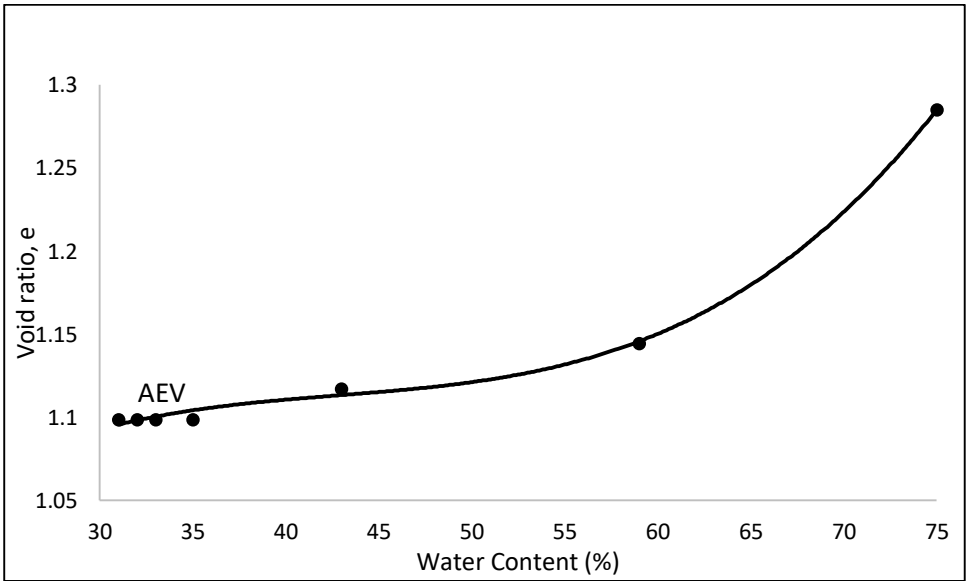

Figure 4.22: Void Ratio Versus Water Content After Swelling of Natural Soil

Test results from shrinkage curve obtained in Figure 4.5 by using air drying method gave an AEV at a water content of 13% whereas by using the drying method with the use of silica gel resulted an AEV value at a water content of 34%.

4.9 Matric Suction Test Result

Figure 4.22 describes the relationship between the gravimetric water content and the matric suction of the natural soil obtained by using the filter paper method. It defines the amount of water that is retained in the soil for a given matric value. The shape and distribution of pores in soil is characterized by the shape of SWCC. From Figure 4.23, it can be seen that the AEV of the specimen was at about 31% water content which is in good harmony with the value of the water content obtained by using the silica gel drying method.

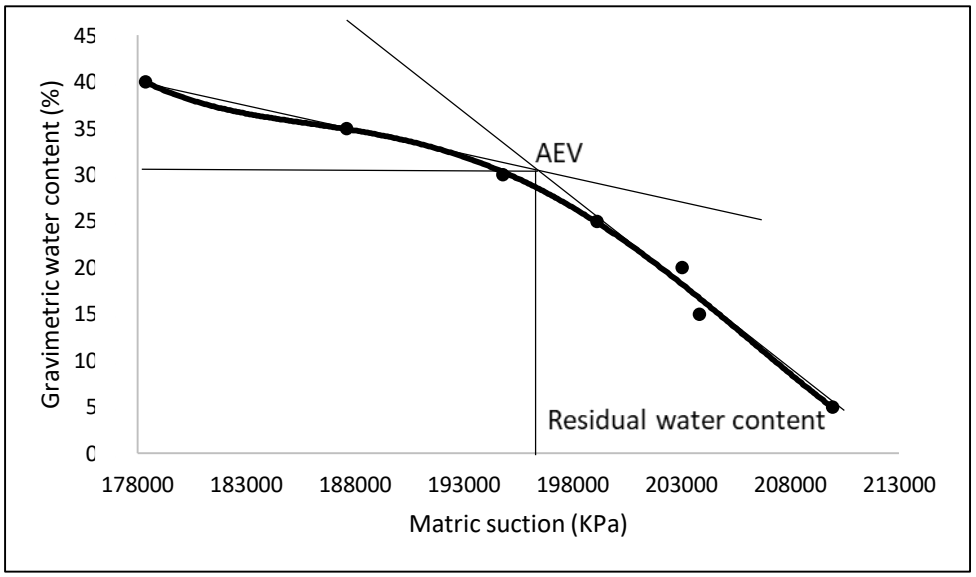

Figure 4.23: Natural Soil Water Characteristics Curve

Chapter 5

CONCLUSIONS

In the study, a series of tests were conducted to evaluate the swelling, shrinkage and cracking properties of the natural and bentonite added soils. Digital image tool was used to analyze the crack intensity factor, CIF for the specimen mixed with 5% and 10% bentonite. The overall results in this research can be summarized as:

- Under the desiccation methods employed in this study which were air drying, oven drying and drying with the use of silica gel, the moisture content of the natural and bentonite added soils decreased with time.
- Air drying method applied on the natural soil did not generate any significant desiccation cracks on the soils whereas for the bentonite added soils, some cracks were observed.
- Desiccation cracks depends on the water present in the soil. As water content decreased, the formation of desiccation cracks increased in bentonite added soils. The constant evaporation stage became stable once the soil moisture content reached the air entry value, AEV. At this point, the soil was transferred from saturated to unsaturated state.
- During the wetting/drying cycles, for soil specimen containing 10% bentonite, the CIF increased continuously with increasing number of cycles whereas for specimen with 5% bentonite, significant increase in the CIF values was obtained up to the end of 3rd cycle and then after that cycle, slight increase in the CIF value was obtained.

- During shrinkage, a decrease in volume of soil is due to evaporation of moisture that exists in its pores. Soil samples oven dried at 60^{o}C temperature has a higher desiccation rate compared to air drying.
- The tensile strength of the natural soil by using the double punch test was obtained at an axial force of 180 N.
- The AEV of the natural soil specimen obtained at a 31% water content from SWCC was in good harmony with the value of the water content obtained from the drying curve by using the silica gel drying method.
- The SWCC curve depicts a well-graded granular material as the suction level decreases with decrease in gravimetric water content.

5.1 Recommendation

In the course of this study, the desiccation cracking behavior of soil with and without bentonite was studied. However, more research still needs to be carried out to understand the cracking behavior. The following developments are recommended as further research:

1. A larger mold can be considered to observe cracks and understand their mechanism with a well robust result.
2. Other crack parameters can be considered in examining the behavior of desiccation cracks.
3. The addition of higher percentages of bentonite to the natural soil can be adopted in order to understand the effect of increasing percentage of active minerals on desiccation cracking.
4. Different methods of tensile strength tests can be adopted and the results can be compared. For better understanding of the effect of bentonite on the tensile

strength, tensile strength tests should also be performed on bentonite added soils.

5. Wetting and drying cycles on different percentages of bentonite added soils should be conducted in order to fully understand the desiccation cracking of bentonite added soils.

REFERENCES

Abedinzadeh, R. (1991). Quantification of particle shape and angularity using the image analyzer. *Geotechnical Testing Journal*, *14*(3), 296-308.

Alawaji, H. A. (1999). Swell and compressibility characteristics of sand–bentonite mixtures inundated with liquids. *Applied Clay Science*, *15*(3-4), 411- 430.

Albrecht, B. A., & Benson, C. H. (2001). Effect of desiccation on compacted natural clays. *Journal of Geotechnical and Geoenvironmental Engineering*, *127*(1), 67-75.

Anderson, M.G., Hubbard, M.G. and Kneale, P.E. (1982) 'The influence of shrinkage cracks on porewater pressures within a clay embankment', Quarterly *Journal of Engineering Geology and Hydrogeology 15*(1), 9-14.

Auvray, R., Rosin-Paumier, S., Abdallah, A., & Masrouri, F. (2014). Quantification of soft soil cracking during suction cycles by image processing. *European journal of environmental and civil engineering*, *18*(1), 11-32.

Avila, G., Ledesma, A., & Lloret, A. (2013). One-dimensional cracking model in clayey soils. In *Proceddings of the 18th International Conference on Soil Mechanics and Geotechnical Engineering* (pp. 1077-1080).

Azadegan, O., Kaffash, A. E., Yaghoubi, M. J., & Pourebrahim, G. R. (2012). Laboratory study on the swelling, cracking and mechanical characteristics of

the palm fiber reinforced clay. *Electronic Journal of Geotechnical Engineering*, *17*, 47-54.

Ba, M., Nokkaew, K., Fall, M., & Tinjum, J. M. (2013). Effect of matric suction on resilient modulus of compacted aggregate base courses. *Geotechnical and Geological Engineering*, *31*(5), 1497-1510.

Barzegar, A. R., Rengasamy, P., & Oades, J. M. (1995). Effects of clay type and rate of wetting on the mellowing of compacted soils. *Geoderma*, *68*(1-2), 39-49.

Bažant, Z. P., & Xiang, Y. (1997). Crack growth and lifetime of concrete under long time loading. *Journal of Engineering Mechanics*, *123*(4), 350-358.

Bradley, C., Mosugu, M., & Gerrard, J. (2007). Seasonal dynamics of soil–water pressure in a cracking clay soil. *Catena*, *69*(3), 253-263.

Bulut, R., Hineidi, S. M., and Bailey, B. (2002). Suction Measurements - Filter Paper and Chilled Mirror Psychrometer," The Proceedings, Texas Section ASCE, Fall Meeting, Waco, Texas.

Bulut, R., Lytton, R. L., & Wray, W. K. (2001). Soil suction measurements by filter paper. In *Expansive clay soils and vegetative influence on shallow foundations* (pp. 243-261).

Cerato, A. B., & Lutenegger, A. J. (2002). Determination of surface area of fine-grained soils by the ethylene glycol monoethyl ether (EGME) method. *Geotechnical Testing Journal*, *25*(3), 315-321.

Chen F.H (1988) *Foundations on Expansive Soils* Elsevier Scientific Publishing Co., Amsterdam.

Chertkov V.Y (2002), Modelling cracking stages of saturated soils as they dry and shrink Eur. J. Soil Sci., 53 (1) pp. 105-118.

Colina, H., & Roux, S. (2000). Experimental model of cracking induced by drying shrinkage. *The European Physical Journal E*, *1*(2-3), 189-194.

Cornelis, W. M., Corluy, J., Medina, H., Diaz, J., Hartmann, R., Van Meirvenne, M., & Ruiz, M. E. (2006). Measuring and modelling the soil shrinkage characteristic curve. *Geoderma*, *137*(1-2), 179-191.

Dakshanamuthy, V., 1978, "A new method to predict swelling using a hyperbolic equation," Geotechnical Engineering, Vol. 9, pp. 79–87.

Daniel, D.E. and Wu, Y.K., 1993, "Compacted clay liners and covers for arid sites," Journal of Geotechnical Engineering, ASCE, Vol. 119, No. 2, pp. 223–237.

Eigenbrod, K. D. (1996). Effects of cyclic freezing and thawing on volume changes and permeabilities of soft fine-gained soils. *Canadian Geotechnical Journal*, *33*(4), 529-537.

Elberling, B. Soil Responses to Climate Change. MDA Rounsevell & PJ Loveland, eds. NATO ASI Series. Series I: Global Envoironmental Change, 23. Springer, Berlin 1994. x, 312 s., ill., 24 cm. DEM 198,-. *Geografisk Tidsskrift.*

Fang, H. Y. (1970). Method of Test for Tensile Strength of Soil, Rock and Stabilized Materials by Double Punch Test, Fritz Laboratory Reports. Paper 1967.

Fang, H. Y. & Chen, W. F. (1971). New Method for Determination of Tensile Strength of Soils, Highway Research Record, No. 345, 62-68.

Fang, H. Y., & Chen, W. F. (1972). Further study of double-punch test for tensile strength of soils. *Proc1 3nd Southeast Asian Conf on Soil Engineering*, *19721*, 236-242.

Fawcett, R. G., & Collis-George, N. (1967). A filter-paper method for determining the moisture characteristics of soil. *Australian Journal of Experimental Agriculture*, *7*(25), 162-167.

Fredlund D.G, Rahardjo H, and Fredlund M.D, (2012). Unsaturated Soil Mechanics in Engineering Practice. John Wiley & Sons. Canada.

Fredlund, D. G. (2002, March). Use of the soil-water characteristic curve in the implementation of unsaturated soil mechanics. In *Proceedings of the 3rd International Conference on Unsaturated Soils, Recife, Brazil* (Vol. 3, pp. 887-902).

Fredlund, D. G., & Rahardjo, H. (1993). *Soil mechanics for unsaturated soils*. John Wiley & Sons.

Fredlund, D. G., and Xing, A. (1994). Equation for the soil water characteristic curve, Canadian Geotechnical Journal, 31: 521-532.

Gavin, K., & Xue, J. (2010). Design charts for the stability analysis of unsaturated soil slopes. *Geotechnical and Geological Engineering*, *28*(1), 79.

Ge L., Yang K.H., 'Tensile strength of lightly cemented sand through indentation tests', *Proceedings of the 18th International Conference* on Soil Mechanics and Geotechnical Engineering, Paris, 2013).

Gray, D. H. (1989). Geotechnical engineering of land disposal systems. In *The Landfill* (pp. 145-173). Springer, Berlin, Heidelberg.

Greacen, E. L., Walker, G. R., & Cook, P. G. (1987). *Evaluation of the filter paper method for measuring soil water suction* (No. 89-111127. CIMMYT.).

Groenevelt, P. H., & Grant, C. D. (2004). Analysis of soil shrinkage data. *Soil and Tillage Research*, *79*(1), 71-77.

Haines WB (1923) The volume changes associated with variations of water content in soil. J Agric Sci 13:296–310.

Hanafy, E.A.D.E. 1991. Swelling/shrinkage characteristic curve of desiccated expansive clays. ASTM Geotechnical Testing Journal, 14(2): 206–211.

Holtz, R. D., Kovacs, W. D., & Sheahan, T. C. (1981). *An introduction to geotechnical engineering* (Vol. 733). Englewood Cliffs, NJ: Prentice-Hall.

Horn, R., & Albrechts, C. (2002). Stress strain effects in structured unsaturated soils on coupled mechanical and hydraulic processes. In *2002 ASAE Annual Meeting* (p. 1). American Society of Agricultural and Biological Engineers.

Hu, L. B., Péron, H., Hueckel, T., & Laloui, L. (2013). Desiccation shrinkage of nonclayey soils: multiphysics mechanisms and a microstructural model. *International Journal for Numerical and Analytical Methods in Geomechanics*, *37*(12), 1761-1781.

Inaudi, D., Laloui, L., & Steinmann, G. (2000). Looking below the surface. *Concrete Engineering International*, *4*(3).

Jotisankasa, A., & Mairaing, W. (2010). Suction-monitored direct shear testing of residual soils from landslide-prone areas. *Journal of geotechnical and geoenvironmental engineering*, *136*(3), 533-537.

Kodikara, J., Barbour, S., & Fredlund, D. G. (2002). Structure development in surficial heavy clay soils: a synthesis of mechanisms. *Australian Geomechanics: Journal and News of the Australian Geomechanics Society*, *37*(3), 25-40.

Kim, H., Prezzi, M., & Salgado, R. (2016). Calibration of Whatman Grade 42 filter paper for soil suction measurement. *Canadian journal of soil science*, *97*(2), 93-98.

Kim, T. H., Kim, C. K., Jung, S. J., & Lee, J. H. (2007). Tensile strength characteristics of contaminated and compacted sand-bentonite mixtures. *Environmental geology*, *52*(4), 653-661.

Klingbeil, N. W. (2003). A total dissipated energy theory of fatigue crack growth in ductile solids. *International Journal of Fatigue*, *25*(2), 117-128.

Kodikara, J. and Costa, S. (2013) 'Desiccation Cracking in Clayey Soils: Mechanisms and Modelling', in Multiphysical Testing of Soils and Shales. Springer, pp. 21-32.

Kodikara, J., Barbour, S., & Fredlund, D. G. (2002). Structure development in surficial heavy clay soils: a synthesis of mechanisms. *Australian Geomechanics: Journal and News of the Australian Geomechanics Society*, *37*(3), 25.

Komine, H. (2004). Simplified evaluation on hydraulic conductivities of sand–bentonite mixture backfill. *Applied Clay Science*, *26*(1-4), 13-19.

Komine H. & Ogata N. (1994). Exprimental study on swelling characteristics of compacted bentonite. *Canadian Geotechnical Journal*, vol. 31, 478-490.

Lakshmikantha, M. R., Prat, P. C., & Ledesma, A. (2009). Image analysis for the quantification of a developing crack network on a drying soil. *Geotechnical Testing Journal*, *32*(6), 505-515.

Leong, E. C., & Wijaya, M. (2015). Universal soil shrinkage curve equation. *Geoderma*, *237*, 78-87.

Leong, E. C., He, L., & Rahardjo, H. (2002). Factors affecting the filter paper method for total and matric suction measurements. *Geotechnical Testing Journal*, *25*(3), 322-333.

Li, Y. N., Hong, A. P., & Bažant, Z. P. (1995). Initiation of parallel cracks from surface of elastic half-plane. *International journal of fracture*, *69*(4), 357-369.

Likos WJ, Lu N (2004) Hysteresis of capillary stress in unsaturated granular soil. J Eng Mech 130(6).ASCE, ISSN0733-9399/2004/ 646–655.

McKeen, R. G. (1980). Field studies of airport pavements on expansive clay. In *Expansive Soils* (pp. 242-261). ASCE.

Miller, C. J., Mi, H., & Yesiller, N. (1998). Experimental analysis of desiccation crack propagation in clay liners 1. *JAWRA Journal of the American Water Resources Association*, *34*(3), 677-686.

Mishra, A.K., Dhawan, S. and Rao, S.M. (2008) 'Analysis of swelling and shrinkage behavior of compacted clays', Geotechnical and Geological Engineering, 26(3),pp. 289-298.

Mishra, P. N., Scheuermann, A., Bore, T., & Li, L. (2019). Salinity effects on soil shrinkage characteristic curves of fine-grained geomaterials. *Journal of Rock Mechanics and Geotechnical Engineering*, *11*(1), 181-191.

Mitchell, J.K. 1993. Fundamentals of Soil Behavior. John Wiley & Sons, New York.

Mitchell, J. K., & Soga, K. (2005). *Fundamentals of soil behavior* (Vol. 3). New York: John Wiley & Sons.

Mokhtari, M., & Dehghani, M. (2012). Swell-shrink behavior of expansive soils, damage and control. *Electronic Journal of Geotechnical Engineering*, *17*, 2673-2682.

Nahlawi, H., & Kodikara, J. K. (2006). Laboratory experiments on desiccation cracking of thin soil layers. *Geotechnical & Geological Engineering*, *24*(6), 1641-1664.

Nelson D.J., Miller J.D. (1992) Expansive Soils: Problems and Practice in Foundation and Pavement Engineering John Wiley & Sons, New York.

Novák, V. (1999) 'Soil-crack characteristics-estimation methods applied to heavy soils in the NOPEX area', Agricultural and Forest Meteorology, 98, pp. 501-507.

Oluwaseun. S. Bamgbopa. (2016). Investigation of shrinkage and cracking in clay soils under wetting and drying cycles. *International Journal of Engineering Research and Technology*, 11(5), 283-285.

Önal, O., Ören, A. H., Özden, G., & Kaya, A. (2008). Determination of Cylindrical Soil Specimen Dimensions by Imaging with Application to Volume Change of Bentonite-Sand Mixtures. *Geotechnical Testing Journal*, *31*(2), 124-131.

Ören, A. H., Önal, O., Özden, G., & Kaya, A. (2006). Nondestructive evaluation of volumetric shrinkage of compacted mixtures using digital image analysis. *Engineering geology*, *85*(3-4), 239-250.

Pande, G. N., & Pietruszczak, S. (2015). On unsaturated soil mechanics–personal views on current research. *Studia Geotechnica et Mechanica*, *37*(3), 73-84.

Peng, X., Horn, R., Peth, S., & Smucker, A. (2006). Quantification of soil shrinkage in 2D by digital image processing of soil surface. *Soil and Tillage Research*, *91*(1-2), 173-180.

Perrier, E., Mullon, C., Rieu, M. and Marsily, G. (1995) 'Computer construction of fractal soil structures: simulation of their hydraulic and shrinkage properties', Water Resources Research, 31(12), pp. 2927-2943.

Power, K. C., Vanapalli, S. K., & Garga, V. K. (2008). A revised contact filter paper method. *Geotechnical Testing Journal*, *31*(6), 461-469.

Preston, S., Griffiths, B. S., & Young, I. M. (1997). An investigation into sources of soil crack heterogeneity using fractal geometry. *European Journal of Soil Science*, *48*(1), 31-37.

Puppala, A. J., Katha, B., & Hoyos, L. R. (2004). Volumetric shrinkage strain measurements in expansive soils using digital imaging technology. *Geotechnical testing journal*, *27*(6), 547-556.

Rao, A.S., Phanikumar, B.R. and Sharma, R.S. (2004) 'Prediction of swelling characteristics of remoulded and compacted expansive soils using free swell index', Quarterly *journal of engineering geology and hydrogeology*, 37(3), pp. 217-226.

Rayhani, M. H., Yanful, E. K., & Fakher, A. (2007). Desiccation-induced cracking and its effect on the hydraulic conductivity of clayey soils from Iran. *Canadian geotechnical journal*, *44*(3), 276-283.

Ridley, A. M., Dineen, K., Burland, J. B., & Vaughan, P. R. (2003). Soil matrix suction: some examples of its measurement and application in geotechnical engineering. *Géotechnique*, *53*(2), 241-253.

Ridley, A., McGinnity, B., & Vaughan, P. (2004). Role of pore water pressures in embankment stability. *Proceedings of the Institution of Civil Engineers-Geotechnical engineering*, *157*(4), 193-198.

Rodríguez Pacheco, RL (2002). Experimental study of flow and transport of chromium, nickel and manganese in residues of the Moa mining area (Cuba): influence of the hydromechanical behavior.

Rounsevell, M. D. A., Evans, S. P., & Bullock, P. (1999). Climate change and agricultural soils: impacts and adaptation. *Climatic Change*, *43*(4), 683-709.

Sánchez, M., Manzoli, O. L., & Guimarães, L. J. (2014). Modeling 3-D desiccation soil crack networks using a mesh fragmentation technique. *Computers and Geotechnics*, *62*, 27-39.

Sarmah, A. K., Pillai-McGarry, U., & McGarry, D. (1996). Repair of the structure of a compacted Vertisol via wet/dry cycles. *Soil and Tillage Research*, *38*(1-2), 17-33.

Shi, B. X., Chen, S., & Zheng, C. (2014). Expansive soil crack depth under cumulative damage. In *Soil Behavior and Geomechanics* (pp. 1-14).

Shi, B. X., Zheng, C. F., & Wu, J. K. (2014). Research progress on expansive soil cracks under changing environment. *The Scientific World Journal*, *2014*.

Shu-Rong Y, Wei-Hsing .H, and Shao-Hung C. (2015). Journal of Marine Science and Technology, Vol. 23, No. 3, pp. 281-287.

Singh, S. P., Rout, S., & Tiwari, A. (2018). Quantification of desiccation cracks using image analysis technique. *International Journal of Geotechnical Engineering*, *12*(4), 383-388.

Sreedeep, S., & Singh, D. N. (2006). Methodology for determination of osmotic suction of soils. *Geotechnical & Geological Engineering*, *24*(5), 1469-1479.

Swarbrick, G. E. (1995). Measurement of soil suction using the filter paper method. In *Proceedings of The First International Conference on Unsaturated Soils/Unsat'95/Paris/France/6-8 September 1995. Volume 2*.

Tang, C., Shi, B., Liu, C., Zhao, L. and Wang, B., (2008) 'Influencing factors of geometrical structure of surface shrinkage cracks in clayey soils', *Engineering Geology*, 101(3), pp. 204-217.

Tang, C.-S., Cui, Y.-J., Shi, B., Tang, A.-M. and Liu, C. (2011) 'Desiccation and cracking behaviour of clay layer from slurry state under wetting–drying cycles', Geoderma 166(1), pp.111-118.

Tang, C.-S., Cui, Y.-J., Tang, A.-M. and Shi, B. (2010) 'Experiment evidence on the temperature dependence of desiccation cracking behavior of clayey soils', Engineering Geology, 114(3), pp. 261-266.

Tiwari, A. (2015). *Quantification of Cracks and Shrinkage Using Image Analysis* (Doctoral dissertation).

Tripathy, S., Rao, K. S., & Fredlund, D. G. (2002). Water content-void ratio swell-shrink paths of compacted expansive soils. *Canadian geotechnical journal*, *39*(4), 938-959.

Vanda, Y. (2014). *Effect of Pore Water Chemistry on Hydro-Mechanical Behavior of Compacted Expansive Clay* (Doctoral dissertation, Eastern Mediterranean University (EMU)-Doğu Akdeniz Üniversitesi (DAÜ)).

Wijaya, M., & Leong, E. C. (2014). Modelling shrinkage behaviour of soft soils. In *Proceedings of softsoils 2014*. Bandung Indonesia.

Yang, S., Huang, W., & Chung, S. (2015). Combined effects of temperature and moisture content on soil suction of compacted bentonite. *Journal of Marine Science and Technology*, *23*, 281-287.

Yao, Y., Tung, S. T. E., & Glisic, B. (2014). Crack detection and characterization techniques—An overview. *Structural Control and Health Monitoring*, *21*(12), 1387-1413.

Yao, Y., Van Tol, A. F., Van Paassen, L. A., & Vardon, P. J. (2014). Shrinkage and swelling properties of flocculated mature fine tailings. In *IOSTC 2014: Proceedings of the 4th International Oil Sands Tailings Conference, Lake Louise, Canada, 7-10 December 2014*. University of Alberta.

Yesiller, N., Miller, C. J., Inci, G. and Yaldo, K. 2000. Desiccation and cracking behavior of three compacted landfill liner soils, *Engineering Geology*, **57**, (1–2), 105–121.

Yong, R. N. (1999). Soil suction and soil-water potentials in swelling clays in engineered clay barriers. *Engineering geology*, *54*(1-2), 3-13.

Yong, R. N., Boonsinsuk, P., & Wong, G. (1986). Formulation of backfill material for a nuclear fuel waste disposal vault. *Canadian Geotechnical Journal*, *23*(2), 216-228.

Zapata, C. E., Houston, W. N., Houston, S. L., & Walsh, K. D. (2000). Soil–water characteristic curve variability. In *Advances in unsaturated geotechnics* (pp. 84-124).